Astronomy & Astrophysics manuscript no. cygnus˙ms
December 10, 2012

A spectroscopic investigation of the O-type star population in four Cygnus OB associations

I. Determination of the binary fraction

L. Mahy[1], G. Rauw[1], M. De Becker[1], P. Eenens[2], and C. A. Flores[2]

[1] Institut d'Astrophysique et de Géophysique, Université de Liège, Bât. B5C, Allée du 6 Août 17, B-4000, Liège, Belgium
e-mail: mahy@astro.ulg.ac.be
[2] Departamento de Astronomía, Universidad de Guanajuato, Apartado 144, 36000 Guanajuato, GTO, Mexico

Received ...; accepted ...

ABSTRACT

Context. Establishing the multiplicity of O-type stars is the first step towards accurately determining their stellar parameters. Moreover, the distribution of the orbital parameters provides observational clues to the way that O-type stars form and to the interactions during their evolution.
Aims. Our objective is to constrain the multiplicity of a sample of O-type stars belonging to poorly investigated OB associations in the Cygnus complex and for the first time to provide orbital parameters for binaries identified in our sample. Such information is relevant to addressing the issue of the binarity in the context of O-type star formation scenarios.
Methods. We performed a long-term spectroscopic survey of nineteen O-type stars. We searched for radial velocity variations to unveil binaries on timescales from a few days up to a few years, on the basis of a large set of optical spectra.
Results. We confirm the binarity for four objects: HD 193443, HD 228989, HD 229234 and HD 194649. We derive for the first time the orbital solutions of three systems, and we confirm the values of the fourth, showing that these four systems all have orbital periods shorter than 10 days. Besides these results, we also detect several objects that show non-periodic line profile variations in some of their spectral lines. These variations mainly occur in the spectral lines, that are generally affected by the stellar wind and are not likely to be related to binarity.
Conclusions. The minimal binary fraction in our sample is estimated to be 21%, but it varies from one OB association to the next. Indeed, 3 O stars of our sample out of 9 (33%) belonging to Cyg OB1 are binary systems, 0% (0 out of 4) in Cyg OB3, 0% (0 out of 3) in Cyg OB8, and 33% (1 out of 3) in Cyg OB9. Our spectroscopic investigation also stresses the absence of long-period systems among the stars in our sample. This result contrasts with the case of the O-type stellar population in NGC 2244 among which no object showed radial velocity variations on short timescales. However, we show that it is probably an effect of the sample and that this difference does not a priori suggest a somewhat different star forming process in these two environments.

Key words. Stars: early-type - Stars: binaries: spectroscopic - Open clusters and associations: individual: Cygnus OB1 - Open clusters and associations: individual: Cygnus OB3 - Open clusters and associations: individual: Cygnus OB8 - Open clusters and associations: individual: Cygnus OB9

1. Introduction

The multiplicity of massive stars constitutes one of the most essential ingredients for understanding these objects. Establishing it is the first step in obtaining valuable physical parameters, such as their masses, radii and luminosities. The binarity also affects the evolutionary paths of the components in such systems in comparison to single stars through phenomena, such as tidal interations or Roche lobe overflows (Sana & Evans 2011). Knowing this multiplicity also allows us to be more accurate on the wind parameters, especially the mass-loss rates, or on the intrinsic X-ray luminosities. Moreover, the distribution of the orbital parameters for the massive systems provides us with additional information on the way that massive close binaries are formed.

Many different scenarios for the formation of these objects have been proposed (see Zinnecker & Yorke 2007, for a complete review), but none of them totally explains what happens during their formation or during its earliest stages. This renders our knowledge of massive stars still fragmentary. In addition, the distribution of orbital parameters allows us to give insight into other avertions such as whether the binary fraction of massive stars can be related to the stellar density (Penny et al. 1993; García & Mermilliod 2001). The orbital parameters of multiple systems can thus provide important clues to the conditions prevailing in the birthplace during their formation or to the dynamical interations that occur during the earliest stages of their evolution. Several studies have already been performed in spectroscopy to determine the binary fraction of O-type stars in nearby young open clusters (see e.g., Sana & Evans 2011, and references therein). All these analyses revealed an averaged binary fraction of about 44±5% (Sana & Evans 2011). However, to investigate such a large parameter space, it is necessary to combine other observation techniques, such as interferometry (Nelan et al. 2004), speckle interferometry (see e.g., Mason et al. 1998; Maíz-Apellániz et al. 2004; Mason et al. 2009), or adaptative optics (Turner et al. 2008). Indeed, all these large surveys give the advantages of better statistics whilst the surveys devoted to young open clusters or OB associations allow more homoge-

Send offprint requests to: L. Mahy

Article published by EDP Sciences, to be cited as http://dx.doi.org/10.1051/0004-6361/201219425

neous stellar populations to be investigated as noted by Kiminki & Kobulnicky (2012).

The Cygnus area is an active star-forming region in the Milky Way. Its relative proximity (0.7 – 2.5 kpc, Uyanıker et al. 2001) makes this region suitable for studying stellar populations and star formation processes (see Reipurth & Schneider 2008, for a review). The Cygnus constellation harbours nine OB associations and at least a dozen of young open clusters. To better constrain the environment of the Cygnus region, Fig.1 represents a schematic view with the locations, in galactic coordinates, of the different OB associations and of several young open clusters. The central association Cyg OB2 is certainly the most famous and one of the youngest of the Cygnus region with Cyg OB8. To be more accurate, Cyg OB2 has in fact been shown to possibly have two populations with ages of 2 – 3.5 and 5 Myrs (Wright et al. 2010), whilst the O stars seem to belong to a younger population, possibly aged about 2 Myrs (Hanson 2003). In its surroundings, the associations Cyg OB1, Cyg OB3, Cyg OB7 and Cyg OB9 are older with ages of about 7.5, 8.3, 13.0 and 8.0 Myrs, respectively (Uyanıker et al. 2001). Though the Cygnus region is rich in O-type stars, its heavy absorption prevents one from obtaining a better estimate of the stellar population even though about 100 hot stars are expected in Cyg OB1, Cyg OB8 and Cyg OB9 together (Mel'Nik & Efremov 1995) and about 100 O-stars are expected only in the Cyg OB2 association (Knödlseder et al. 2002; Comerón et al. 2002). However, the membership of certain massive stars to a given cluster or association is sometimes not clearly defined due to the complexity of this area. Recent investigation of the multiplicity of massive stars in Cyg OB2 association performed by Kiminki et al. (2012, and subsequent papers) has shown that the hard minimum binary fraction for the massive stars in this association is estimated at 21%. Such an investigation for the massive star population in the other OB associations in the Cygnus complex is currently lacking.

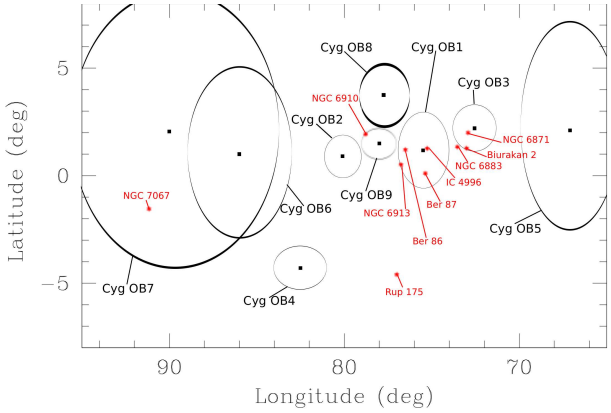

Fig. 1. Schematic view of the different OB associations and young open clusters in the Cygnus region.

We have undertaken a long-term spectroscopic survey of nineteen O-type stars sampled over four different OB associations (Cyg OB1, Cyg OB3, Cyg OB8 and Cyg OB9) as well as in several young open clusters belonging to these associations (e.g., Berkeley 86, NGC 6871, NGC 6913,...). Their membership to a given association or cluster is established on the basis of the catalogue of Humphreys (1978). However, many other O-type stars belong to these associations but we only focus on these targets because they are relatively bright and their binary status was not yet subject to a detailed spectroscopic study, except for HD 229234. We will also include other stars already known as binaries in the discussions on the binary fraction in the different Cygnus OB associations. Moreover, the majority of the objects investigated in the present paper were poorly observed in the past mainly due to the high extinction towards the Cygnus region. In this context, this paper (the first of a series of two) aims at establishing the multiplicity as well as the spectral classification of these stars. This analysis focuses on other regions in the Cygnus complex than the large survey of Kiminki et al. (2012, and the subsequent papers) which was devoted to the Cyg OB2 association. Therefore, this analysis can thus be seen as a complement to the study of the binary fraction in Cygnus region.

The present paper is organized as follows. The observing campaign is described in Sect. 2. The binary status of the stars in our sample is discussed in the next four sections according to the different OB associations. Section 3 is devoted to O-type stars in the Cyg OB1 association, Sect. 4 to these objects in Cyg OB3, Sect. 5 to Cyg OB8, and Sect. 6 to Cyg OB9. Finally, Sect. 7 discusses the observational biases and the binary fraction that we determine whilst Sect. 8 summarizes our results.

2. Observations and binary criteria

Deriving the binary fraction of a given population requires an intense survey of the stars but also a good time sampling to constrain the short- as well as the long-period systems. This monitoring has to be as homogeneous as possible because combining data from the literature may provide erroneous results. Indeed, the literature (especially the older papers) often does not specify on which spectral line the radial velocities (RVs) were measured. Therefore, large differences can be observed between RVs measured on two different lines of a presumably single star. This can lead to some overdeterminations of the spectroscopic binary fraction as notably observed in García & Mermilliod (2001) for the young open cluster IC 1805 (Rauw & De Becker 2004; De Becker et al. 2006; Hillwig et al. 2006). Moreover, it is important to keep in mind the possible observational biases that can prevent the detection of a binary system. Therefore, stars for which no evidence of binarity is found can never be definitely considered as single. Even if no RV shift is detected, the system could be seen under a particular orientation, have a very long period or perhaps a high eccentricity, thereby making the RV variations not significant over a long timescale.

We performed a spectroscopic survey spread over three years (from 2008 to 2011) of all the nineteen stars of our sample, except for HD 194280 which was observed between 2004 and 2007 (see Table 1). This selection of stars however constitutes another observational bias because we limited our observations to stars bright enough to yield good quality data with exposure times not longer than one hour with 1.5 or 2-meter class telescopes. Considering the high – and heterogeneous – extinction towards the Cygnus region, the present monitoring of O-type stars (among which some could also be member of multiple systems) is far from being complete. Nevertheless, we collected a set of 274 spectra for these nineteen stars by using three different instruments. Table 1 lists the stars and the parameters of the observing runs. Table 2, available electronically, gives the Heliocentric Julian Dates (HJD) and the RVs measured on different spectral lines for all the observations. For the SB2 systems, the RVs refined by cross-correlation are also provided. In the latter table as in the following of the present paper, HJD is expressed in format HJD – 2 450 000 for readability. Our dataset thus allowed us to study the RV and line profile variations in the

observed spectra over short- (a few days) and long-term (a few years) timescales.

A first part of our dataset was obtained with the Aurélie spectrograph at the 1.52m telescope at Observatoire de Haute-Provence (OHP, France). The spectra are obtained with a resolving power of about $R = 9\,000$, they are centred on 4650 Å and cover wavelengths between 4450 Å and 4900 Å. However, for some spectra of HD 193443, another configuration of the instrument was chosen. In this case, the resolving power was equal to $R = 12000$, these spectra are centred on 4550 Å and cover 4450 to 4650 Å. Typical exposure times between 25 and 60 min yielded spectra with a signal-to-noise ratio larger than 150 as measured in the continuum close to 4800 Å. The data reduction procedure, performed with the MIDAS software, is described in Rauw & De Becker (2004).

Another part of the data was collected with the ESPRESSO spectrograph mounted on the 2.12m telescope at Observatorio Astronómico Nacional of San Pedro Màrtir (SPM) in Mexico. This échelle spectrograph provides spectra spread over 27 orders, covering a wavelength domain between 3780 Å and 6950 Å with a spectral resolving power of $R = 18\,000$. Typical exposure times ranged from 15 to 30 min. We combined the consecutive exposures of an object in a given night to obtain signal-to-noise ratios close to 150. As a result, our time series did not allow us to investigate RV variations with timescales shorter than 0.8 day, which is not a problem for multiplicity investigations as typically the shortest periods for massive stars are longer than one day (as Kepler's third law would imply orbital separations smaller than the radii of the components for such short periods). The data were reduced using the échelle package available within the MIDAS software.

We also retrieved eight spectra taken before 2008 from the Elodie archives to complete our dataset. Elodie was an échelle spectrograph, mounted at the 1.93m telescope at OHP, with 67 orders in the [3850 – 6850] Å spectral domain and a resolving power of $R = 42\,000$.

We fit one or two Gaussian profiles on several strong spectral lines to estimate the RVs of the stars when the line profiles were not too much broadened by rotation. For the rapid rotators ($v \sin i \geq 300$ km s^{-1}), we used a synthetic line profile broadened with the projected rotational velocity of the star to measure the Doppler shifts by least square. This RV analysis is performed by using the rest wavelengths quoted by Conti et al. (1977) for the [4000 – 5000] Å wavelength domain and Underhill (1994) for wavelengths above 5000 Å. The common wavelength region between the majority of the data is [4450 – 4900] Å. In this spectral band, some interstellar lines exist but they are not sufficiently strong and narrow to use them as indicators of the RV uncertainties. Our previous experience with the same spectrographs (see Mahy et al. 2009) showed that a standard deviation on the RVs of about 7 – 8 km s^{-1} is commonly achieved with these spectra. We therefore consider the RV changes as significant when the standard deviations computed from the RV measurements reach at least this value. For rapid rotators, we consider them as variable if standard deviations of at least 15 km s^{-1} are determined. We stress that the threshold value for the rapid rotators has been increased relative to Mahy et al. (2009) because the present data are slightly noisier. As a consequence, we consider, in the present paper, that a star is an SB1 binary system if the RV variations are significant (i.e., the standard deviation is at least larger than 7 – 8 km s^{-1} for the slow and mid rotators and at least 15 km s^{-1} for rapid rotators) and periodic. We are dealing with an SB2 if the signature of a companion whose spectral lines move in anti-phase with those of the main star is observed. Moreover, if in the cases where significant variations of the RVs are measured on all the spectral lines without any periodic motion, the object will be labelled as a "binary candidate". Finally, we also calculate the Temporal Variance Spectrum (TVS, Fullerton et al. 1996) to search for line profile variations. The TVS provides quantitative information of the temporal variability as a function of the wavelength. If the variations exceed the threshold we can reject the null hypothesis of non-variability of the spectral lines. When such variations are detected for *all* the line profiles, the TVS may then be considered as an additional indicator of multiplicity and, in this case, the star is reported as binary candidate.

The SB2 binary systems detected in the present work are analysed as follows. After having measured the RVs of both components, we use these values as an input of our disentangling programme. This programme is based on the González & Levato (2006) technique and it allows us to compute the individual spectra of both components, and to refine the RVs by applying a cross-correlation technique. It is thus possible to obtain more reliable RVs at phases where the spectral lines are heavily blended. The cross-correlation windows used for the RV determinations generally gather the strongest helium lines (He I 4471, He II 4542, He II 4686 and He I 4713) for both components. With these refined RVs, we then apply the Heck-Manfroid-Mersch method (hereafter HMM, Heck et al. 1985, revised by Gosset et al. 2001) to the time series of $RV_S - RV_P$ to determine the orbital period of the system. The 1-σ error-bar on the period is estimated by assuming an uncertainty on the frequency of the peak associated to the orbital period equal to 10 % of the natural width of the peaks in the Fourier power spectrum (e.g., $\Delta\nu \sim (10\,\Delta T_{\rm tot})^{-1}$, where $\Delta T_{\rm tot}$ is the time elapsed between the first and the last observations of our campaign). The orbital period is then used to determine the orbital solution of the system by applying the Liège Orbital Solution Package (LOSP[1]). To finish the analysis of the systems, we estimate, from the spectral classification of each component, the spectroscopic brightness ratio of the system. For that purpose, we compute the mean ratios between the observed equivalent widths (EWs) and the "canonical" EWs for stars with same spectral classifications as those of the components of binary systems. These "canonical" values are taken from Conti & Alschuler (1971) and Conti (1973). In addition, we associate these values to EWs measured from synthetic spectra of stars having also similar spectral classifications. The 1-σ error-bar given on the brightness ratio corresponds to the dispersions of the ratios measured on each spectral line. This brightness ratio is essential to correct the disentangled spectra in order that they are comparable to those of single stars.

Finally, for all the O-type stars of our sample, we also derive their spectral type. For that, we use the quantitative criteria of Conti & Alschuler (1971), Conti (1973) and Mathys (1988, 1989). These criteria rely on the EW ratio of diagnostic lines. These EWs are measured on the highest signal-to-noise spectra of each objects. We adopt, in the present paper, the following usual notations: $\log W' = \log(EW_{4471}) - \log(EW_{4542})$ for the spectral type, $\log W'' = \log(EW_{4089}) - \log(EW_{4143})$ and $\log W''' = \log(EW_{4388}) + \log(EW_{4686})$ for the luminosity class. However, the $\log W''$ criterion is restricted to O 7 – O 9.7 stars whilst the $\log W'''$ can only be used for O 8 – O 9.7 stars. To be applicable, this last criterion requires that the stars be single

[1] This program, maintained by H. Sana, is available at http://www.science.uva.nl/~hsana/losp.html and is based on the generalization of the SB1 method of Wolfe et al. (1967) to the SB2 case along the lines described in Rauw et al. (2000) and Sana et al. (2006).

or that the brightness ratio between both components be known. The uncertainties on the spectral type determination are generally of about one temperature and luminosity class. To complete this classification, we also use the “f tag” notation presented by Walborn (1971) and the subsequent papers.

Table 1. List of stars investigated in this study. ΔT corresponds to the time elapsed between the first and the last observation of an observing run and is expressed in days, and N represents the number of spectra for each star.

Stars	Cyg	Obs. run	Instrument	Wavelength domain	ΔT	N
HD 193443	Cyg OB1	Aug. 2004	OHP - Elodie/1.93m	[3850 – 6850]Å	–	1
		Aug. 2005	OHP - Elodie/1.93m	[3850 – 6850]Å	–	1
		Sep. 2008	OHP - Aurélie/1.52m	[4450 – 4900]Å	7.06	4
		Oct. 2008	OHP - Aurélie/1.52m	[4450 – 4900]Å	3.17	3
		Dec. 2009	OHP - Aurélie/1.52m	[4450 – 4650]Å	2.98	3
		Jun. 2010	OHP - Aurélie/1.52m	[4450 – 4900]Å	19.98	13
		Aug. 2010	OHP - Aurélie/1.52m	[4450 – 4900]Å	5.94	7
		Dec. 2010	OHP - Aurélie/1.52m	[4450 – 4650]Å	4.00	5
HD 193514	Cyg OB1	Aug. 2004	OHP - Elodie/1.93m	[3850 – 6850]Å	–	1
		Aug. 2005	OHP - Elodie/1.93m	[3850 – 6850]Å	–	1
		Sep. 2008	OHP - Aurélie/1.52m	[4450 – 4900]Å	7.17	4
		Oct. 2008	OHP - Aurélie/1.52m	[4450 – 4900]Å	4.07	5
		Jun. 2009	SPM - Espresso/2.12m	[3780 – 6950]Å	–	1
		Jun. 2010	OHP - Aurélie/1.52m	[4450 – 4900]Å	5.83	6
		Aug. 2010	OHP - Aurélie/1.52m	[4450 – 4900]Å	4.93	4
HD 193595	Cyg OB1	Sep. 2008	OHP - Aurélie/1.52m	[4450 – 4900]Å	7.13	4
		Oct. 2008	OHP - Aurélie/1.52m	[4450 – 4900]Å	1.14	2
		Jun. 2009	SPM - Espresso/2.12m	[3780 – 6950]Å	–	1
		Aug. 2010	OHP - Aurélie/1.52m	[4450 – 4900]Å	4.00	2
HD 193682	Cyg OB1	Sep. 2008	OHP - Aurélie/1.52m	[4450 – 4900]Å	7.02	4
		Oct. 2008	OHP - Aurélie/1.52m	[4450 – 4900]Å	1.06	2
		Jun. 2009	SPM - Espresso/2.12m	[3780 – 6950]Å	–	1
		Jun. 2010	OHP - Aurélie/1.52m	[4450 – 4900]Å	–	1
		Aug. 2010	OHP - Aurélie/1.52m	[4450 – 4900]Å	2.98	2
HD 194094	Cyg OB1	Jun. 2009	SPM - Espresso/2.12m	[3780 – 6950]Å	3.93	2
		Aug. 2010	OHP - Aurélie/1.52m	[4450 – 4900]Å	4.94	2
		Sep. 2011	SPM - Espresso/2.12m	[3780 – 6950]Å	–	1
HD 194280	Cyg OB1	Oct. 2004	OHP - Aurélie/1.52m	[4450 – 4900]Å	4.05	3
		Jun. 2005	OHP - Aurélie/1.52m	[4450 – 4900]Å	8.03	7
		Sep. 2006	OHP - Aurélie/1.52m	[4450 – 4900]Å	4.07	8
		Oct. 2006	OHP - Aurélie/1.52m	[4450 – 4900]Å	–	1
		Nov. 2007	OHP - Aurélie/1.52m	[4450 – 4900]Å	26.95	23
HD 228841	Cyg OB1	Sep. 2008	OHP - Aurélie/1.52m	[4450 – 4900]Å	6.08	3
		Oct. 2008	OHP - Aurélie/1.52m	[4450 – 4900]Å	–	1
		Jun. 2009	SPM - Espresso/2.12m	[3780 – 6950]Å	–	1
		Jun. 2010	OHP - Aurélie/1.52m	[4450 – 4900]Å	–	1
		Aug. 2010	OHP - Aurélie/1.52m	[4450 – 4900]Å	3.18	2
HD 228989	Cyg OB1	Aug. 2009	SPM - Espresso/2.12m	[3780 – 6950]Å	0.80	2
		Jul. 2010	SPM - Espresso/2.12m	[3780 – 6950]Å	–	1
		Aug. 2010	OHP - Aurélie/1.52m	[4450 – 4900]Å	5.13	5
		Jun. 2011	SPM - Espresso/2.12m	[3780 – 6950]Å	3.94	5
		Sep. 2011	SPM - Espresso/2.12m	[3780 – 6950]Å	1.98	5
HD 229234	Cyg OB1	Sep. 2008	OHP - Aurélie/1.52m	[4450 – 4900]Å	1.06	2
		Oct. 2008	OHP - Aurélie/1.52m	[4450 – 4900]Å	1.82	2
		Jun. 2009	SPM - Espresso/2.12m	[3780 – 6950]Å	–	1
		Aug. 2009	SPM - Espresso/2.12m	[3780 – 6950]Å	0.96	2
		Jun. 2010	OHP - Aurélie/1.52m	[4450 – 4900]Å	6.06	4
		Jul. 2010	SPM - Espresso/2.12m	[3780 – 6950]Å	1.06	2
		Aug. 2010	OHP - Aurélie/1.52m	[4450 – 4900]Å	5.86	6
HD 190864	Cyg OB3	Aug. 2001	OHP - Elodie/1.93m	[3850 – 6850]Å	–	1
		Sep. 2008	OHP - Aurélie/1.52m	[4450 – 4900]Å	7.05	5
		Oct. 2008	OHP - Aurélie/1.52m	[4450 – 4900]Å	3.25	3
		Jun. 2009	SPM - Espresso/2.12m	[3780 – 6950]Å	5.91	2
		Jun. 2010	OHP - Aurélie/1.52m	[4450 – 4900]Å	1.00	2
		Aug. 2010	OHP - Aurélie/1.52m	[4450 – 4900]Å	4.00	4
HD 227018	Cyg OB3	Sep. 2008	OHP - Aurélie/1.52m	[4450 – 4900]Å	7.05	4
		Oct. 2008	OHP - Aurélie/1.52m	[4450 – 4900]Å	4.02	4
		Aug. 2010	OHP - Aurélie/1.52m	[4450 – 4900]Å	2.02	2
HD 227245	Cyg OB3	Aug. 2009	SPM - Espresso/2.12m	[3780 – 6950]Å	0.86	2

Table 1. continued.

Stars	Cyg	Obs. run	Instrument	Wavelength domain	ΔT	N
		Jun. 2011	SPM - Espresso/2.12m	[3780 – 6950]Å	3.81	3
HD 227757	Cyg OB3	Jun. 2009	SPM - Espresso/2.12m	[3780 – 6950]Å	4.98	2
		Jul. 2010	SPM - Espresso/2.12m	[3780 – 6950]Å	–	1
		Jun. 2011	SPM - Espresso/2.12m	[3780 – 6950]Å	3.94	3
HD 191423	Cyg OB8	Aug. 2004	OHP - Elodie/1.93m	[3850 – 6850]Å	–	1
		Sep. 2008	OHP - Aurélie/1.52m	[4450 – 4900]Å	7.09	4
		Oct. 2008	OHP - Aurélie/1.52m	[4450 – 4900]Å	–	1
		Jun. 2009	SPM - Espresso/2.12m	[3780 – 6950]Å	–	1
		Aug. 2010	OHP - Aurélie/1.52m	[4450 – 4900]Å	3.17	2
HD 191978	Cyg OB8	Aug. 2001	OHP - Elodie/1.93m	[3850 – 6850]Å	1.05	2
		Sep. 2008	OHP - Aurélie/1.52m	[4450 – 4900]Å	5.94	3
		Oct. 2008	OHP - Aurélie/1.52m	[4450 – 4900]Å	–	1
		Jun. 2009	SPM - Espresso/2.12m	[3780 – 6950]Å	8.92	2
		Aug. 2010	OHP - Aurélie/1.52m	[4450 – 4900]Å	4.11	3
HD 193117	Cyg OB8	Sep. 2008	OHP - Aurélie/1.52m	[4450 – 4900]Å	6.82	3
		Oct. 2008	OHP - Aurélie/1.52m	[4450 – 4900]Å	–	1
		Jun. 2009	SPM - Espresso/2.12m	[3780 – 6950]Å	5.05	2
		Aug. 2010	OHP - Aurélie/1.52m	[4450 – 4900]Å	3.20	2
HD 194334	Cyg OB9	Sep. 2008	OHP - Aurélie/1.52m	[4450 – 4900]Å	6.75	2
		Oct. 2008	OHP - Aurélie/1.52m	[4450 – 4900]Å	–	1
		Jun. 2009	SPM - Espresso/2.12m	[3780 – 6950]Å	–	1
		Aug. 2009	SPM - Espresso/2.12m	[3780 – 6950]Å	0.87	2
		Jun. 2010	OHP - Aurélie/1.52m	[4450 – 4900]Å	1.07	2
		Jul. 2010	SPM - Espresso/2.12m	[3780 – 6950]Å	1.03	2
		Aug. 2010	OHP - Aurélie/1.52m	[4450 – 4900]Å	3.87	1
HD 194649	Cyg OB9	Jun. 2009	SPM - Espresso/2.12m	[3780 – 6950]Å	–	1
		Aug. 2009	SPM - Espresso/2.12m	[3780 – 6950]Å	–	1
		Jun. 2010	OHP - Aurélie/1.52m	[4450 – 4900]Å	5.95	3
		Aug. 2010	OHP - Aurélie/1.52m	[4450 – 4900]Å	2.13	2
		Jun. 2011	SPM - Espresso/2.12m	[3780 – 6950]Å	3.93	5
		Sep. 2011	SPM - Espresso/2.12m	[3780 – 6950]Å	3.98	5
HD 195213	Cyg OB9	Sep. 2008	OHP - Aurélie/1.52m	[4450 – 4900]Å	6.96	3
		Oct. 2008	OHP - Aurélie/1.52m	[4450 – 4900]Å	–	1
		Aug. 2009	SPM - Espresso/2.12m	[3780 – 6950]Å	0.96	2
		Jun. 2010	OHP - Aurélie/1.52m	[4450 – 4900]Å	–	1
		Jul. 2010	SPM - Espresso/2.12m	[3780 – 6950]Å	–	1
		Aug. 2010	OHP - Aurélie/1.52m	[4450 – 4900]Å	4.91	2

3. O-type stars in the Cyg OB1 association

3.1. Gravitationally bound systems

3.1.1. HD 193443

Reported as binary by Muller (1954), this star has never been the target of an intense spectroscopic monitoring. Therefore, no orbital solution is known for the system nor are there spectral classifications for the components. We acquired thirty-seven spectra of HD 193443 from Aug 2004 (HJD = 3246.4777) to Dec 2010 (HJD = 5543.2387). These data reveal a periodic variation of the line profiles, clearly visible in the He I 4471 and He I 4713 lines. Even though the signature of the secondary is detected, the small RV separation between both components prevents us from completely resolving the individual line profiles throughout the orbit. The secondary's lines are thus never totally separated from those of the primary even for the helium lines or the metallic lines as it is shown in the upper panel of Fig. 2.

The analysis of the SB2 system is performed as explained in Section 2. However, the Gaussian fit is made on the bottom of the absorption lines of the primary component. At the maximum of the RV separation, we also fit a second profile to determine the RVs of the secondary. The HMM technique measured on the RVs refined by the disentangling programme yields a period of 7.467 ± 0.003 days. From this period, we compute the orbital parameters of HD 193443 listed in Table 3 and the best fit of the RV curves, shown in Fig. 2, is obtained for a non-zero eccentricity.

The study of the disentangled spectra of HD 193443 shows that the He II 4542 line is present but is weak for both components relative to the He I 4471 line. This indicates two late O-type stars. We compute, from the observed spectra, $\log W' = 0.321$ and $\log W' = 0.483$ for the primary and the secondary, respectively, thereby corresponding to respective subtypes of O 9 and O 9.5. However, our dataset does not allow us to constrain the luminosity classes of these stars. Indeed, the majority of our data does not cover the Si IV 4089 and He I 4143 lines. Moreover, for those that do, the RV separation is insufficient to resolve with accuracy the signature of the secondary component and thus to correctly fit it with Gaussian profiles. To determine the brightness ratio, we measure the EWs of the He I 4471, 4713 and He II 4542 lines of the disentangled and observed spectra at the maximum of separation and we compare these values with those of Conti & Alschuler (1971) for stars of the same spectral types as both components. Moreover, we also measure the EWs of the above-quoted lines on synthetic spectra with the same spectral classifications as explained in Section 2. Even though the luminosity class is unknown for both components of HD 193443, the lines that we selected for this computation are only slightly affected by the luminosity class of the stars. Therefore, we decide to take into account the "canonical" EWs of all the stars with only similar subtypes. The ratios of these values provide a brightness ratio of about 3.9 ± 0.4 between the primary and the secondary components. The disentangled spectra, corrected from the brightness ratio, are shown in Fig. 3.

The properties of both components thus show two stars with relatively close spectral types but with large mass and brightness ratios. This indicates that the primary is rather evolved relative to the secondary. First, we assume that HD 193443 is either an O 9III+O 9.5V or an O 9I+O 9.5III system. In the former case, the comparison between the minimum masses and the values quoted in Martins et al. (2005, 22 $M_\odot$ and 16 $M_\odot$ for the primary and the secondary, respectively) suggests an inclination between 17° and 21°. In the latter case, we obtain, from masses estimated to 30 $M_\odot$ for the primary and 21 $M_\odot$ for the secondary, an inclination between 15° and 19°. Therefore, we consider that the inclination of the system is very low and probably ranges between 15° and 22°. From the formula of Eggleton (1983), we compute the projected Roche lobe radii ($RRL \sin i$) of 8.3 $R_\odot$ and 5.6 $R_\odot$

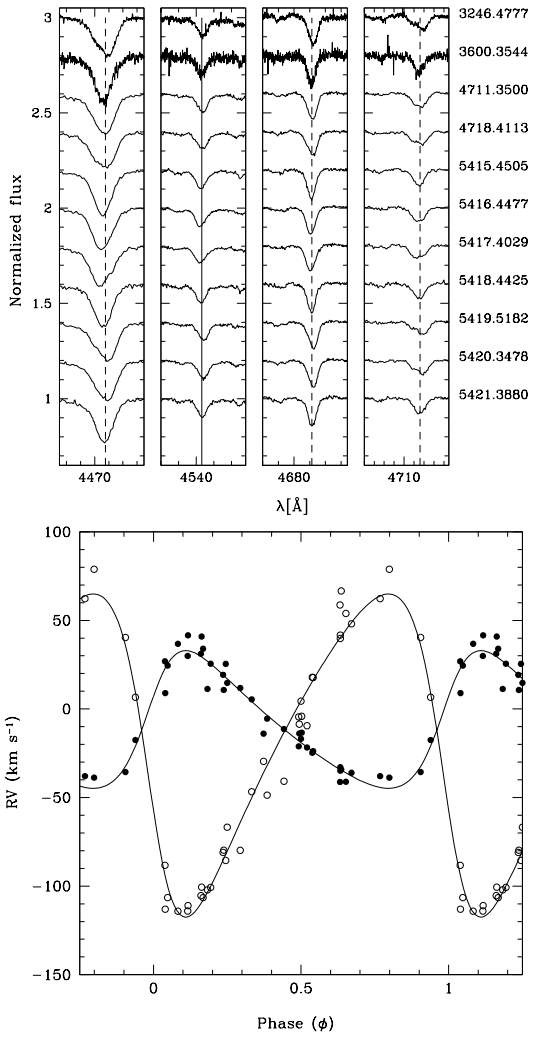

Fig. 2. *Top:* He I 4471, He II 4542, He II 4686, He I 4713 line profiles of HD 193443 at different epochs. *Bottom:* RV curves of HD 193443 computed for a period of 7.467 days. Filled circles represent the primary RVs whilst the open circles correspond to the secondary.

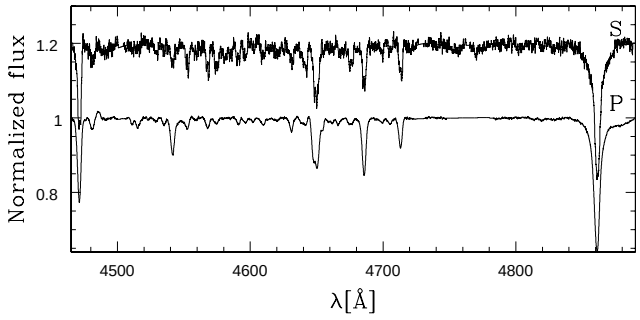

Fig. 3. Disentangled spectra of the two components of HD 193443. The spectra are normalized accounting for the optical brightness ratio of 3.9. The secondary spectrum is vertically shifted for clarity.

Table 2. Journal of the spectroscopic observations of the O-type stars. The first column gives the HJD at mid-exposure. The following columns provide, for each spectral line, the measured RVs (in km s^{-1}). The full table is available at the CDS.

					HD 190864					
HJD	He I 4471	He II 4542	N III 4634	N III 4641	He II 4686	He I 4713	He I 5876	Na I 5889	Na I 5895	Disent
− 2 450 000	[km s^{-1}]	[km s^{-1}]	[km s^{-1}]	[km s^{-1}]	[km s^{-1}]	[km s^{-1}]	[km s^{-1}]	[km s^{-1}]	[km s^{-1}]	[km s^{-1}]
2134.4733	−13.0	−5.2	−19.3	−26.3	−4.9	−18.6	−13.9	−19.1	−18.3	–
4711.3132	−16.4	−7.7	−23.4	−29.5	11.6	−20.9	–	–	–	–
4712.3000	−15.5	−4.3	−20.5	−24.8	13.4	−11.9	–	–	–	–
4712.3111	−13.7	−7.2	−30.3	−24.2	18.0	−15.7	–	–	–	–
4717.2954	−16.0	−6.9	−18.9	−28.4	17.1	−16.6	–	–	–	–
4718.3637	−15.9	−3.9	−19.7	−35.9	13.4	−14.2	–	–	–	–
4740.2629	−15.8	−8.5	−20.5	−30.9	10.9	−18.3	–	–	–	–
4741.3195	−11.0	−5.1	−18.1	−28.3	11.7	−9.6	–	–	–	–
4743.5116	−12.2	−6.5	−15.7	−28.2	13.0	−13.2	–	–	–	–
4982.8779	−20.7	−9.2	−28.3	−62.0	−3.5	−25.4	−13.3	−20.1	−18.6	–
4988.7847	−16.1	−0.8	−10.6	−32.4	−27.7	–	−19.7	−18.4	−18.5	–
5355.4081	−17.0	−4.0	−16.2	−25.1	1.0	−16.1	–	–	–	–
5356.4053	−14.3	−7.2	−17.3	−34.0	−1.2	−14.1	–	–	–	–
5415.3437	−14.0	−5.2	−21.6	−29.5	4.5	−14.8	–	–	–	–
5416.3784	−18.8	−10.9	−25.0	−33.6	−7.0	−20.2	–	–	–	–
5417.3323	−18.5	−8.2	−24.3	−34.4	7.6	−16.9	–	–	–	–
5419.3479	−13.8	−7.1	−20.4	−30.7	0.4	−16.9	–	–	–	–
					HD 227018					
4711.3323	12.7	23.3	–	–	24.4	15.0	–	–	–	–
4712.3346	20.2	23.8	–	–	27.6	21.1	–	–	–	–
4717.3188	16.0	20.9	–	–	25.3	15.0	–	–	–	–
4718.3862	16.4	22.5	–	–	23.6	13.6	–	–	–	–
4740.2871	12.1	15.3	–	–	20.6	13.4	–	–	–	–
4741.3477	12.0	15.8	–	–	16.8	—	–	–	–	–
4742.2887	11.9	19.5	–	–	22.7	16.4	–	–	–	–
4744.3032	15.6	21.6	–	–	22.8	13.0	–	–	–	–
5417.3604	18.2	26.2	–	–	27.1	17.0	–	–	–	–
5419.3755	20.8	27.7	–	–	26.7	24.5	–	–	–	–

for the primary and the secondary components. These values indicate Roche lobe radii between 22 $R_\odot$ and 32 $R_\odot$ for the primary and between 15 $R_\odot$ and 22 $R_\odot$ for the secondary. In both cases, the secondary (which would have a radius of 7 $R_\odot$ or 13 $R_\odot$ depending on the case) and the primary (with a radius between 13 $R_\odot$ and 22 $R_\odot$) would not fill their Roche lobe. Secondly, if the stellar classifications were O 9I for the primary and O 9.5V for the secondary, the values of the inclination would be estimated between 15° and 21°, thereby implying Roche lobe radii between 23 $R_\odot$ and 32 $R_\odot$ for the primary and 16 $R_\odot$ and 22 $R_\odot$ for the secondary. In this case, the primary could fill its Roche lobe. At this stage and for the other SB2 systems, it is important to note that the analysis of the orbital parameters and the estimation of the inclination of the SB2 systems are only made to give a first idea of the geometry of the systems. However, we must be careful on the information provided here. Indeed, the masses given in the tables of Martins et al. (2005) are standard values that also depend on other parameters such as e.g., $\log g$, $T_{\rm eff}$ and/or $\log(L/L_\odot)$. The values quoted in these tables can thus be different from the real parameters of both components. Therefore, it is common that the mass ratios computed from these standard values do not correspond to the real mass ratios determined from the orbital solutions.

3.1.2. HD 228989

Located in the Berkeley 86 young open cluster (Forbes 1981), this star was quoted as an O 9.5+O 9.5 binary system by Massey et al. (1995). However, no orbital solution of this object was yet determined.

We collected eighteen observations of this object between Aug 2009 (HJD = 5049.9519) and Sep 2011 (HJD = 5815.6460). These data clearly reveal, as it is shown in the upper panel of Fig. 4, a binary system composed of two stars with rather similar spectral classifications. Our analysis of the refined RVs gives an orbital period of 1.77352 days. We compute from this value the orbital parameters reported in Table 3. We have computed two orbital solutions: an eccentric and a circular. The rms being smaller for the circular orbit, we decide to fix the eccentricity to zero. The RV curves computed with LOSP are shown in the lower panel of Fig. 4. As suggested from the disentangled spectra and the mass ratio, the two components seem to be quite close to each other in terms of the physical properties. From the raw (i.e., not corrected by the brightness ratio) disentangled spectra and the observed spectra, we determine spectral types of O 8.5 ($\log W' = 0.238$) and O 9.7 ($\log W' = 0.791$) for the primary and the secondary components, respectively. In addition, we obtain, on the most deblended spectra, for the primary $\log W'' = 0.027$ and for the secondary $\log W'' = 0.104$, suggesting a main-sequence luminosity class for both components. Knowing the spectral classifications of these two stars, we estimate a brightness ratio of about 1.2 ± 0.1, the primary being slightly brighter than its companion. This brightness ratio coupled with the luminosities listed in tables of Martins et al. (2005) seem to agree with the luminosity classes of both components. Finally, we display in Fig. 5 the disentangled spectra corrected for the relative brightness.

The comparison between the minimum masses and the masses published by Martins et al. (2005, 19 $M_\odot$ and < 17 $M_\odot$ for the primary and the secondary, respectively) suggests that the system would have an inclination between 42° and 50°. We stress however that the O 9.7 subtype is not included in the table of Martins et al. (2005). Therefore, we consider the values of the O 9.5 subtype as an upper limit. On the basis of Eggleton's formula (1983), we estimate $RRL \sin i$ of about 5.7 $R_\odot$ and 5.3 $R_\odot$ for the primary and the secondary components. From the inclination range estimated from the masses, we compute a Roche lobe radius between 7.4 $R_\odot$ and 8.4 $R_\odot$ for the primary and between 7.0 $R_\odot$ and 8.0 $R_\odot$ for the secondary. Such values seem to

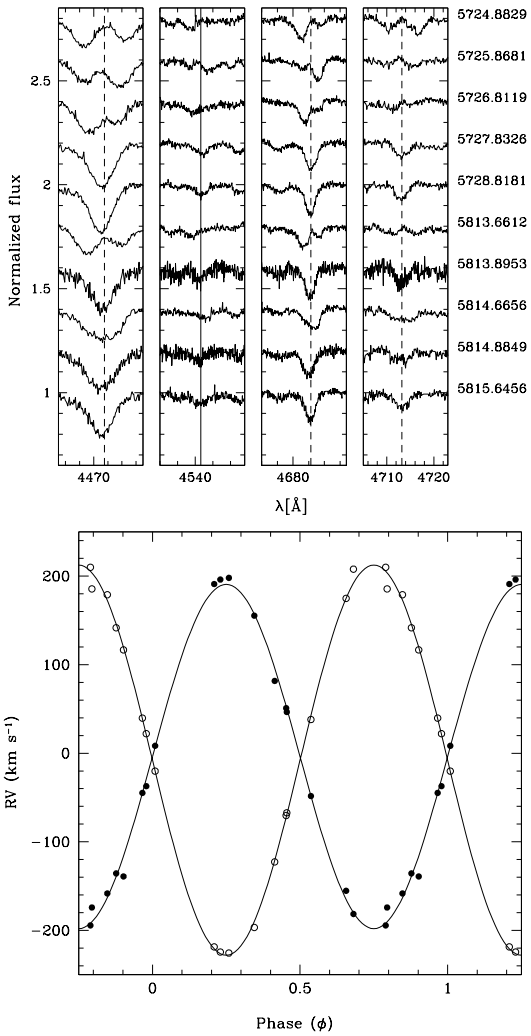

Fig. 4. *Top:* He I 4471, He II 4542, He II 4686, He I 4713 line profiles at different epochs. *Bottom:* RV curves of HD 228989 computed from $P_{\rm orb}$ = 1.77352 days. Filled circles represent the primary whilst the open circles correspond to the secondary.

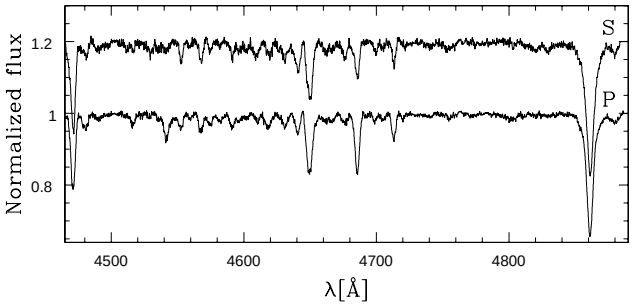

Fig. 5. Disentangled spectra of the two components of HD 228989. The spectra are normalized accounting for a brightness ratio of 1.2. The secondary spectrum is vertically shifted for clarity.

indicate that both components are very close to fill their Roche lobe (standard radii are of 7.9 $R_\odot$ and < 7.2 $R_\odot$ for the primary and the secondary, respectively).

3.1.3. HD 229234

Quoted as belonging to NGC 6913 (Humphreys 1978), HD 229234 was classified as an O 9If star by Massey et al. (1995) whilst Negueruela (2004) reported an O 9II classification and Morgan et al. (1955) reported this star as O 9.5III. Previous investigations of Liu et al. (1989) and Boeche et al. (2004) proposed this star to be a binary system with an orbital period of 3.5105 days. In addition, Boeche et al. (2004) published the first SB1 orbital solution for this star. This SB1 binary status was moreover confirmed by a recent analysis of Malchenko & Tarasov (2009).

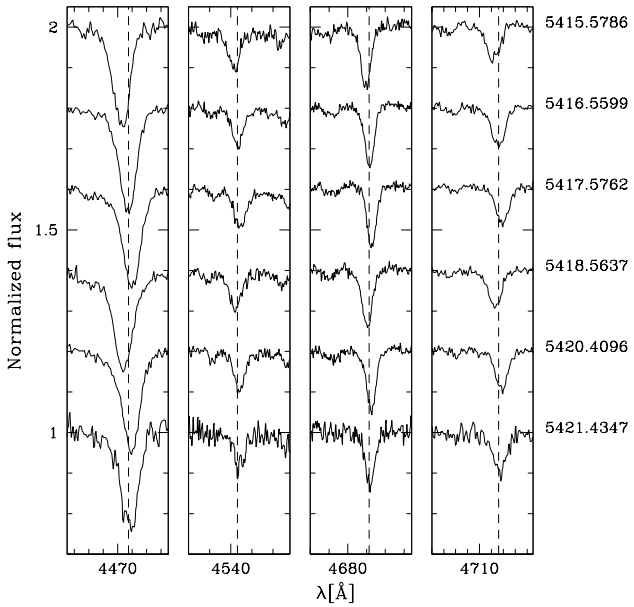

Fig. 6. Short-term variations of the He I 4471, He II 4542, He II 4686 and He I 4713 line profiles of HD 229234. The rest wavelengths are given by the dashed lines.

We obtained nineteen spectra of HD 229234 between Sep 2008 (HJD = 4717.3892) and Aug 2010 (HJD = 5421.4347). This object obviously displays significant variations in its RVs on a short timescale. Fig. 6 shows the Doppler shifts of several spectral lines for six consecutive nights. The periodic motion is clearly visible for all the spectral lines. The mean radial velocities ($\overline{\mathrm{RVs}}$) ± the standard deviation computed from the RVs are −8.7 ± 33.8, 4.9 ± 34.4, 1.7 ± 36.5 and −6.5 ± 34.0 km s^{-1} for the He I 4471, He II 4542, He II 4686 and He I 4713 lines, respectively. No SB2 signature was found in the optical data. We determine on the basis of the HMM technique an orbital period of 3.510595 ± 0.000245 days, agreeing with the previous estimates of Liu et al. (1989) and Boeche et al. (2004). The parameters of the SB1 orbital solution are listed in Table 3 and the RV curve is displayed in Fig. 7. These parameters are globally close to those obtained by Boeche et al. (2004). With the absence of uncertainties in the orbital solution given by these authors, the comparison remains however difficult. The main difference is regardless observed in T_0 value because of a different definition of the phase $\phi = 0.0$.

We also derive, for the main component of this SB1 system, an O 9III classification from the different EW ratios $\log W' = 0.372$, $\log W'' = 0.280$ and $\log W''' = 5.325$. This spectral type appears to be in agreement with the different classifications found in the literature. Unlike Massey et al. (1995), our classification is not only based on a visual comparison with spectra of the atlas of Walborn & Fitzpatrick (1990), but also relies on quantitative values.

From the mass of the primary (22.0 ± 3.0 $M_\odot$ Martins et al. 2005) and the f_{mass} value given in Table 3, we determine, as minimum mass for the secondary component of the system, a value of about 3.0 ± 0.3 $M_\odot$.

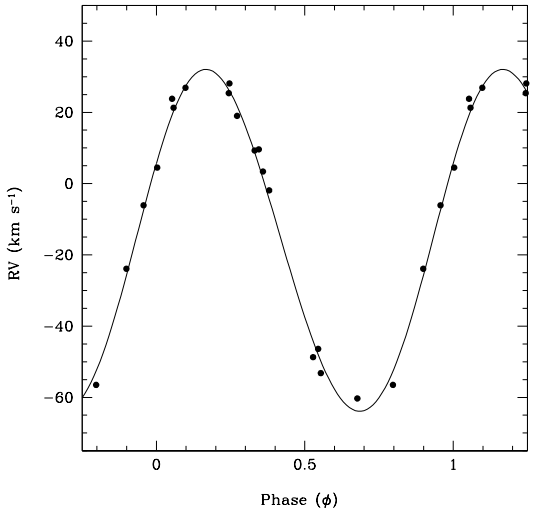

Fig. 7. RV curve of HD 229234 computed from P_{orb} = 3.510595 days.

3.2. Presumably single stars

3.2.1. HD 193514

This star was classified as O 7Ib(f) by Repolust et al. (2004). These authors also reported on a weak emission in the He II 4686 line profile. Changes from day to day were already observed by Underhill (1995) in the Hα profile. However, none of these authors did attribute these variations to a binary nature.

The twenty-two spectra of HD 193514 taken from Aug 2004 (HJD = 3246.5202) to Aug 2010 (HJD = 5420.4585) do not confirm any significant RV variations. The upper parts of Fig. 8 show that the Doppler shifts of the spectral lines are rather small (undetectable by eye) on several (short and long) timescales. We indeed determine $\overline{\mathrm{RVs}}$ = −18.0 ± 5.2, −7.0 ± 5.0 and −15.6 ± 5.0 km s^{-1} for the He I 4471, He II 4542 and He I 4713 lines. In the lower parts of Fig. 8, we show the TVS computed for these different spectral lines. The variations above the dotted lines are considered as significant under a significance level of 1%. Therefore, we see that the TVS of the He II 4542 and the He I 4713 line profiles do not show any substantial variations, though the He I 4471 and especially the He II 4686 lines do. However, since this variability is not detected on all the line profiles, we conclude that it is unlikely to be due to binarity but rather arises in the stellar wind itself. However, we do not have enough échelle spectra to characterize the changes reported by Underhill (1995) in the line profile of Hα. We therefore consider HD 193514 as a presumably single star.

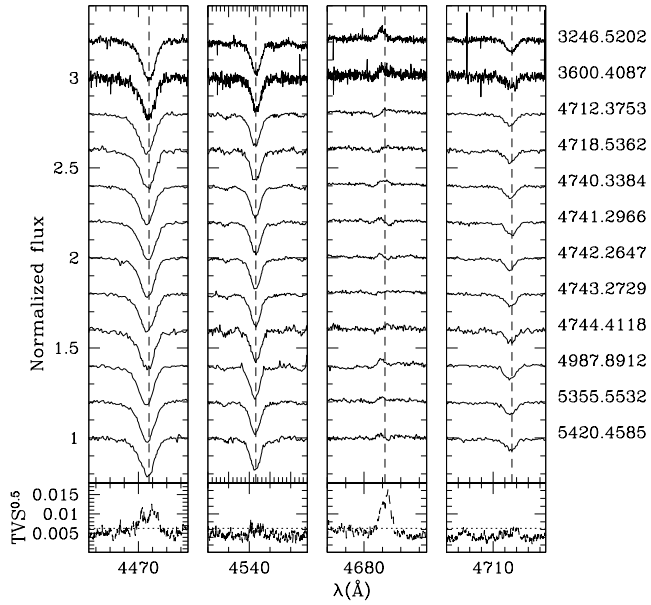

Fig. 8. The He I 4471, He II 4542, He II 4686 and He I 4713 line profiles of HD 193514 according to HJD. The rest wavelengths are given by the dashed lines. At the bottom, TVS of each spectral line computed from the Aurélie data. The dotted line illustrates the 1% significance level for the variability evaluated following the approach of Fullerton et al. (1996).

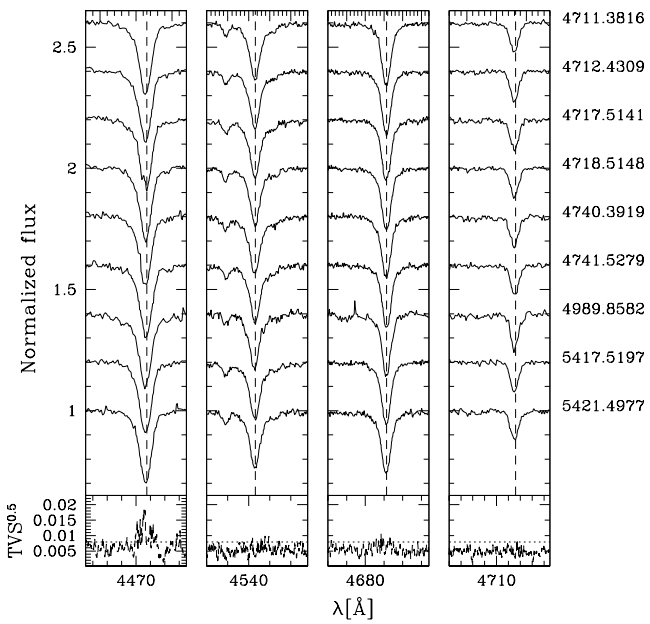

Fig. 9. Same as Fig. 8 but for HD 193595.

From the échelle spectra, we determine $\log W' = 0.014$ and $\log W'' = 0.253$, yielding for HD 193514 a spectral type O 7–O 7.5 and a luminosity class similar to a giant (III). The strong N III 4634–41 lines coupled with the He II 4686 line (for which the emission component is similar to the absorption one) suggest an (f) suffix, which agrees with a giant luminosity class. Therefore, we classify HD 193514 as an O 7–O 7.5 III(f) star.

3.2.2. HD 193595

HD 193595 is located in the Berkeley 86 young open cluster (Massey et al. 1995). Classified as an O 6V (Garmany & Vacca 1991), this object was poorly investigated in terms of RV.

We measure the RVs on nine spectra taken at different epochs, between Sep 2008 (HJD = 4711.3816) and Aug 2010 (HJD = 5421.4977). These data reveal rather constant RVs for this star: $\overline{\mathrm{RVs}} = -13.7 \pm 2.2$, -8.1 ± 2.8, -4.5 ± 2.6 and -12.5 ± 1.7 km s^{-1} for the He I 4471, He II 4542, He II 4686 and He I 4713 lines, respectively. We detect, as shown in the lower panels of Fig. 9, low amplitude variations (at a significance level of 1%) only in the TVS spectrum of the He I 4471 line. The results of the TVS associated to the RV measurements thus seem to imply that the observed variations are probably not due to binarity. By assuming a single status for this object, we derive for HD 193595 an O 7V stellar classification ($\log W' = -0.036$ and $\log W'' = 0.052$).

3.2.3. HD 193682

This star is the hottest object in our sample. HD 193682 seems to have a spectral type oscillating between O 5 (Hiltner 1956) and O 4 (O 4III(f), Garmany & Vacca 1991). We obtained ten spectra of this object between Sep 2008 (HJD = 4711.4038) and Aug 2010 (HJD = 5418.5280). These data show rather broad line profiles, indicating a rather large projected rotational velocity. We determine from the Fourier transform method of Simón-Díaz & Herrero (2007) a $v \sin i = 150$ km s^{-1} for this object. This moderately fast rotation yields broader lines that produce larger uncertainties on their centroid and hence poorer accuracy of the RVs. However, we do not perform a least-square fit with a synthetic profile broadened by rotation to determine the RVs of this star because the shapes of the strongest lines are still Gaussian. We determine $\overline{\mathrm{RVs}}$ of about -48.6 ± 11.3, -39.7 ± 7.7 and -55.1 ± 11.1 km s^{-1} for the He I 4471, He II 4542 and He II 4686 lines, respectively. Such a high 1-σ dispersion is probably due to the line broadening rather than to binary motion because this RV dispersion is smaller on the strongest spectral lines. Furthermore, we do not detect any secondary signature in the observed spectra nor any change of the line width as a function of time, as it is shown in the upper panels of Fig. 10. Indeed, we see from this figure that the spectral lines have always their centre at the same side of the dashed lines, which represent the rest wavelengths. We compute the TVS for these spectral lines (lower panels of Fig. 10) and we find a significant (although weak) variation in the line profile of He II 4686, a spectral line generally affected by strong stellar winds. We cannot consider these changes as due to binarity because they are not detected in all the spectral lines, notably in the He I 4471 and the He II 4542 lines, which suggest that these variations are probably intrinsic to the stellar wind rather than attributable to a putative companion.

We then calculate, from the He I 4471–He II 4542 ratio, $\log W' = -0.514$, corresponding to an O 5 subtype. Furthermore, Walborn's criterion suggests to add a (f) suffix, indicating a moderate emission for the N III 4634−41 lines and a moderate absorption for the He II 4686 line, similar to giant (III) stars. To summarize, we classify HD 193682 as an O 5III(f) star. This spectral classification is similar to those found in the literature.

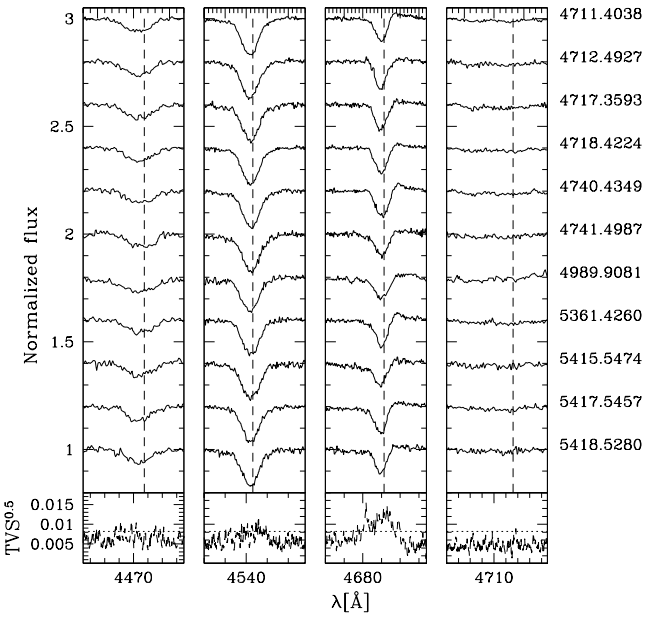

Fig. 10. Same as Fig. 8 but for HD 193682.

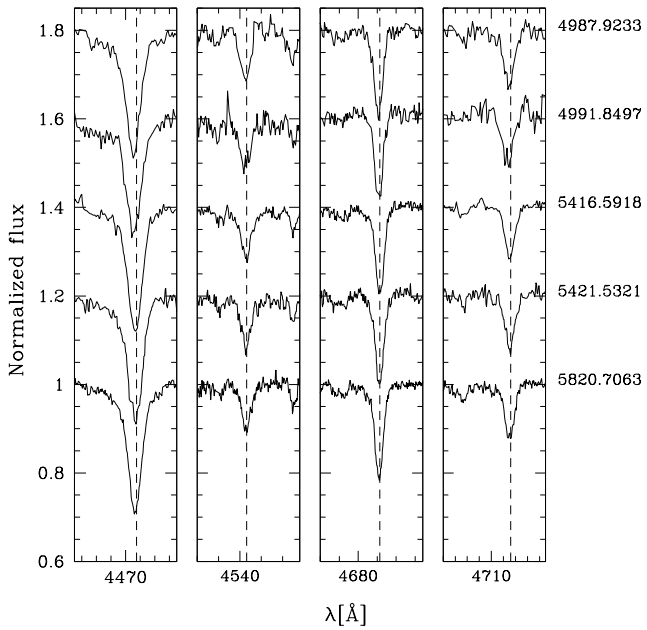

Fig. 11. The He I 4471, He II 4542, He II 4686 and He I 4713 line profiles of HD 194094.

3.2.4. HD 194094

During our spectroscopic campaign, HD 194094 was only observed 5 times: twice in Jun 2009, twice in Aug 2010 and once in Sep 2011. These data however allow us to investigate RV variations on timescales from one week to one year. These five spectra do not exhibit any evidence of a putative companion on such timescales nor any periodic motion relative to the rest wavelengths (dashed lines in Fig. 11). We measure the RVs on the He I 4471, He II 4542, He II 4686 and He I 4713 lines, reporting $\overline{\mathrm{RVs}} = -18.2\pm3.9, -11.3\pm3.8, -9.7\pm8.9$ and -13.9 ± 6.1 km s^{-1}, respectively. The standard deviations on these measurements indicate that HD 194094 is probably single and that the RV variations detected on the He II 4686 line are likely due to a variable stellar wind. However, unlike the stars previously analysed, the Aurélie data for HD 194094 are not sufficiently numerous nor sufficiently spread over the entire campaign to compute the TVS. We also cannot include the SPM data in the computation of the TVS, as we would need to convolve the data so that they all have the same resolution. Indeed, unlike HD 46150 in Mahy et al. (2009), we do not have, in the [4450 – 4900] Å wavelength domain, diagnostic lines similar to the interstellar Na I lines at 5890 Å and 5896 Å to compare the convolved spectra.

Finally, by assuming that this object is single, we compute, from an échelle spectrum of HD 194094, $\log W' = 0.232$, $\log W'' = 0.174$ and $\log W''' = 5.204$, yielding an O 8.5III star. This spectral type is slightly earlier than reported in the literature (O 9III, Hiltner 1956). However, the error-bars on the determination of the spectral type do not allow us to claim that the new classification is significantly different from the older ones.

3.2.5. HD 194280

Presented as a prototype of the OC 9.7Iab class, HD 194280 appears to be a carbon-rich star with a depletion in nitrogen (Goy 1973; Walborn & Howarth 2000). According to these authors, the profiles of He I 5876 and Hα would indicate that the stellar wind is weak.

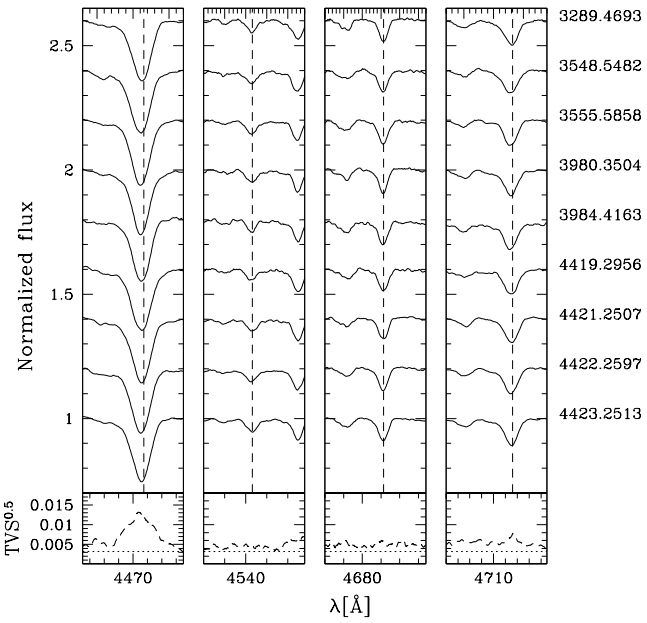

Fig. 12. Sample of spectra taken from the entire dataset. This figure is similar to Fig. 8 but for HD 194280.

We obtained forty-two spectra of this target with the Aurélie spectrograph in the [4450 – 4900] Å wavelength domain between Oct 2004 (HJD = 3286.3646) and Nov 2007 (HJD = 4423.2513). The spectral lines sampled over different timescales are displayed in the upper panels of Fig. 12. This figure shows that the Doppler shifts of the lines are small, which is confirmed by the $\overline{\mathrm{RVs}}$. These values for the He I 4471, He II 4542, He II 4686 and He I 4713 lines are indeed equal to -24.9 ± 4.2, -11.6 ± 7.6, -5.4 ± 5.0 and -17.1 ± 4.8 km s^{-1}, respectively, suggesting that this star is presumably single. From the He I 4471–He II 4542 ratio, we obtain $\log W' = 0.742$, which agrees with the O 9.7 sub-

type. Furthermore, the object presents strong line-profile variations notably in the He I 4471 line. The results of the TVS are shown in the lower panels of Fig. 12. Since the profile of the He II 4686 line does not appear in emission and since the profiles of the He I 5876 and Hα lines did not seem to indicate strong stellar wind (Goy 1973), these variations are unlikely due to the wind. Therefore, another possible explanation for this strong variability in He I 4471 could be pulsations.

3.2.6. HD 228841

Massey et al. (1995) located this object in the Berkeley 86 young open cluster, along with HD 193595 and HD 228989. This star was successively classified as O 7V((f)) and O 6.5Vn((f)) by Massey et al. (1995) and Sota et al. (2011, and references therein).

Eight optical spectra were collected from Sep 2008 (HJD = 4712.3982) to Aug 2010 (HJD = 5418.5980), mainly in the [4450 – 4490] Å range. The spectra show broad lines which means that HD 228841 is likely a rapid rotator. We indeed see, in the upper panels of Fig. 13, that the spectral line widths remain constant as a function of time, which does not seem to support the presence of a secondary component. Therefore, we determine from the Fourier transform method of Simón-Díaz & Herrero (2007) the projected rotational velocity of the star. We obtain a value of 317 km s^{-1}. The mean RVs determined by least-square fit between a rotation profile and the spectral lines amount to $\overline{\mathrm{RVs}} = -48.4 \pm 8.9$, -25.5 ± 6.5 and -44.9 ± 25.3 km s^{-1} for the He I 4471, He II 4542 and He I 4713 lines, respectively. Given the $v \sin i$, the standard deviations generally smaller than 15 km s^{-1} favour a single status for this object. In addition, the variations in the line profiles computed with the TVS (see the lower panels of Fig. 13) are not significant, which agrees with the presumably single status for HD 228841. The high dispersion detected for the He I 4713 line is probably due to the weakness of this line.

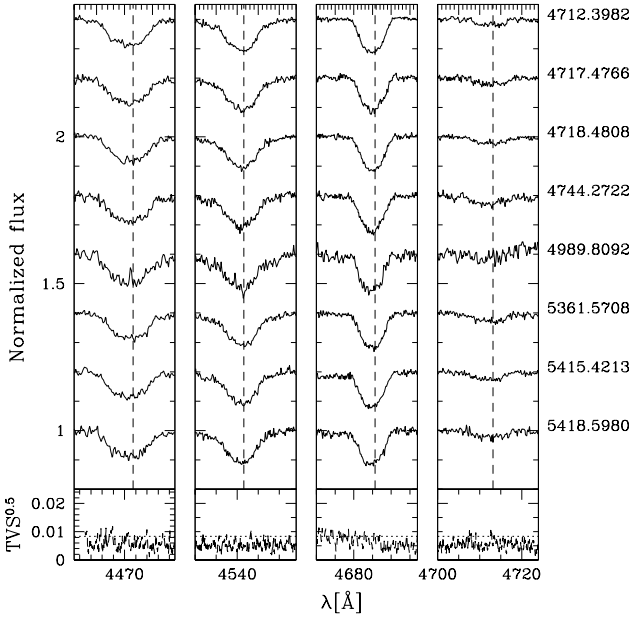

Fig. 13. Same as Fig. 8 but for HD 228841.

We then derive the spectral type of this star from Conti's criterion. $\log W'$ is equal to -0.011, which indicates an O 7 star, as already determined by Massey et al. (1995). We stress however that $\log W''$ could not be estimated given the broadness of the lines and thus the severe blend of the Si IV 4089 line with Hδ.

4. O-type stars in the Cyg OB3 association

4.1. Presumably single stars

4.1.1. HD 190864

Quoted as belonging to NGC 6871 (Humphreys 1978), HD 190864 is one of the brightest O-type stars of Cyg OB3. The spectral classifications derived for this object range between O 6 (Hiltner 1956) and O 7 (Conti & Leep 1974) but agree on a giant luminosity class. Previous investigations (e.g., Plaskett 1924) quoted this star as SB1 but no solution for its orbital motion has been published. Meisel (1968) listed this star as visual double star with $\Delta m = 0.5$ (O 6+B 0.5Vp). Although these authors did not mention the angular separation, an B 0.5Vp spectral type could match with the spectral type of HD 227586 located at 1′ from HD 190864. More recently, Garmany & Stencel (1992) attributed to HD 190864 a spectral type of B 1II+O 6.5III(f), assigning it an SB2 status. However, it is possible that the B 1II component is the visual component reported by Meisel (1968). Indeed, the latter author also mentioned that the estimate of the luminosity class of the B component was uncertain and could be higher, thereby could be attributed to the B 1II component of Garmany & Stencel (1992). From seven observations spread over two years, Underhill (1995) did however not detect any significant RV variations. According to this author, it is unlikely that the difference between the projected rotational velocity given by Conti & Ebbets (1977, 69 km s^{-1}) and that of Herrero et al. (1992, 105 km s^{-1}) is due to a possible varying blend of the profiles of two putative components but rather seems to originate from an emission component in some absorption lines.

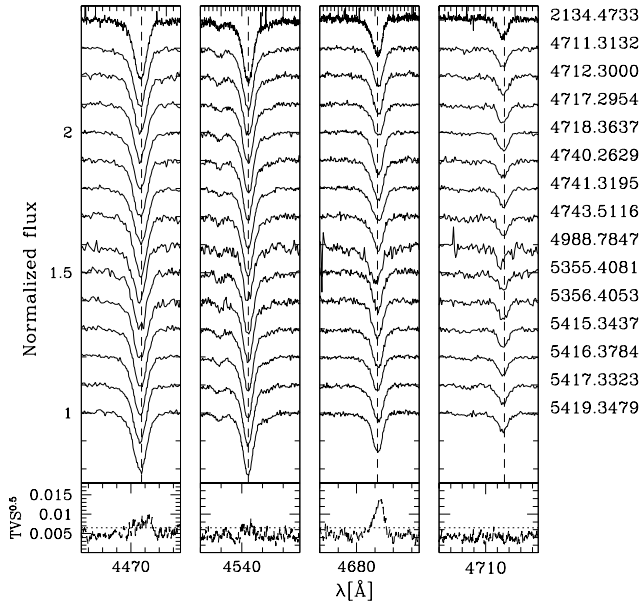

Fig. 14. Same as Fig. 8 but for HD 190864.

We obtained seventeen spectra between Aug 2001 (HJD = 2134.4733) and Aug 2010 (HJD = 5419.3479). This dataset

does not show any significant RV changes, except for the He II 4686 line. The mean RV and the standard deviation measured on this line are indeed of $\overline{RV} = 4.6 \pm 11.5$ km s^{-1} whilst the other values derived on the He I 4471, He II 4542 and He I 4713 lines amount to $\overline{RVs} = -15.5 \pm 2.5$, -6.3 ± 2.4 and -16.5 ± 3.8 km s^{-1}, respectively. Since our observations cover both short and long timescales, we can exclude that HD 190864 is a binary system with an orbital period shorter than about 3000 days. From an intense survey devoted to HD 190864, we have never detected the signature of a putative companion. If a B component was present in the spectrum of HD 190864, we should see it. According to Schmidt-Kaler (1982), a B 0.5V or a B 1II component should be only 6 times fainter than an O 6.5III(f) star and the mass ratio should be between 1 and 4. Therefore, such a component should be visible in the observed spectra, which is not the case. It is thus unlikely that the difference between the two values of $v \sin i$, given by Conti et al. (1977) and Herrero et al. (1992), originates from binarity. Furthermore, if we consider that the RV published by Conti et al. (-15.3 km s^{-1}, 1977) was measured on a He I line, this could constitute an additional clue that the star is presumably single. This thus reveals the importance of a homogeneous dataset to study the binary fraction of massive star populations (as mentioned in Sect. 2).

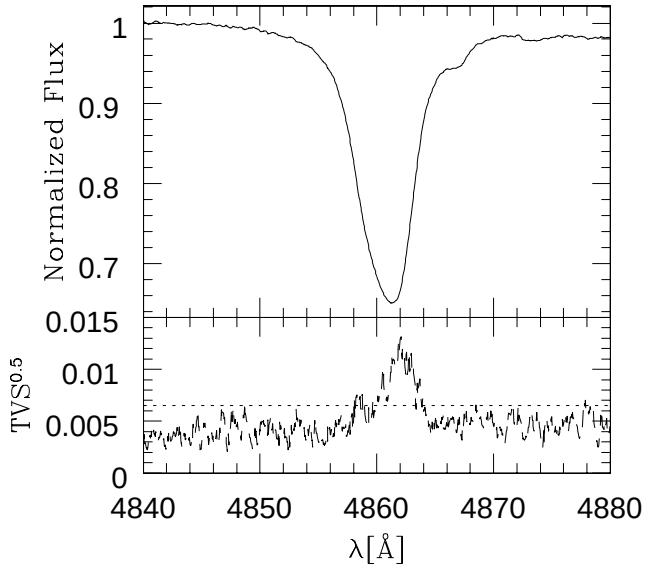

Fig. 15. Mean spectrum and TVS of HD 190864 computed from the Aurélie data of the Hβ line. The dotted line illustrates the 1% significance level for the variability evaluated following the approach of Fullerton et al. (1996).

Though no signature of a secondary companion is found in the HD 190864 spectrum, the TVS analysis reveals significant variations of some line profiles, mainly in the red wings of the He II 4686 and Hβ lines (lower panels of Figs. 14, and Fig. 15). It is however unlikely that these variations are due to the existence of a secondary star. If that was the case, the variability pattern should be once again observed in all the spectral lines which is clearly not the case. Therefore, we classify this object as presumably single.

Finally, we derive from Conti's criterion a spectral classification of O 6.5 ($\log W' = -0.193$), consistent with the previous estimates. The presence of moderate emission in the N III 4634–41 lines and a rather weak He II 4686 line suggest to add the (f) suffix. Therefore, we derive that the spectral classification for HD 190864 is O 6.5III(f).

4.1.2. HD 227018

Located at about 1.2° south-west of HD 190864, HD 227018 is rather faint ($V = 8.98$) for our survey. While its spectral type is relatively well known (O 6.5–O 7), its luminosity class is poorly constrained. Indeed, Herrero et al. (1992) quoted this star as an O 6.5III while Massey et al. (1995) attributed it an O 7V((f)) type.

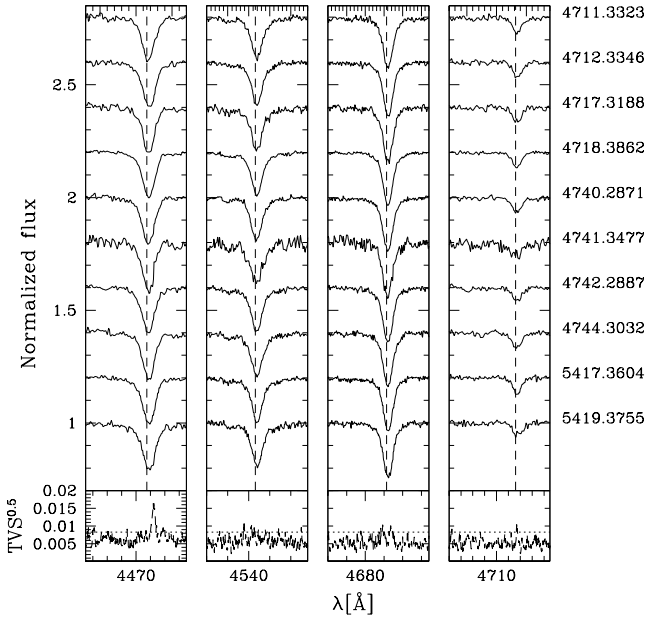

Fig. 16. Same as Fig. 8 but for HD 227018.

Between Sep and Oct 2008, we collected eight spectra with the Aurélie spectrograph and we increased our dataset with two additional spectra taken in August 2010 with the same instrument. The measurements of the RVs reveal rather constant values with $\overline{RVs} = 15.6 \pm 3.4$, 21.7 ± 4.0, 23.8 ± 3.3 and 16.6 ± 3.9 km s^{-1} for the He I 4471, He II 4542, He II 4686 and He I 4713 lines, respectively. We see from the upper panels of Fig. 16 that the Doppler shifts of the spectral lines are relatively small relative to the rest wavelengths. Moreover, the TVS spectra (lower panels of Fig. 16) only exhibit small variations in the He I 4471 line at the limit of being significant while the other lines are relatively stable, thereby indicating that HD 227018 is presumably single. In order to derive the spectral type of this star, we compute, from the He I–He II ratio, $\log W' = -0.201$ which corresponds to an O 6.5 star. We add the ((f)) suffix reminiscent of a main-sequence star because the object shows weak N III 4634–41 emissions and strong He II 4686 absorption lines. Therefore, we classify this star as O 6.5V((f)).

4.1.3. HD 227245

HD 227245 is known as an O 7V (Garmany & Vacca 1991) but its multiplicity has never been investigated until now. From five observations taken between Aug 2009 (HJD = 5049.8148) and Jun 2011 (HJD = 5727.7497), we determine $\overline{RVs} = 5.9 \pm 5.4$,

9.8 ± 3.9, 10.8 ± 6.2 and 6.0 ± 7.3 for the He I 4471, He II 4542, He II 4686 and He I 4713 lines, respectively. Figure 17 shows these spectral lines at different HJD. We stress that a normalization problem occurs at HJD = 5723.9405 for the He I 4471 line but it does not affect the determination of the RV for this line. The standard deviations computed from the RVs are not considered significant because they are generally smaller (except for He I 4713) than the 7 – 8 km s^{-1} threshold defined as our variability criterion. The exception for the He I 4713 line can be explained by the weakness of this line and the signal-to-noise ratio of the data. HD 227245 is thus considered as presumably single.

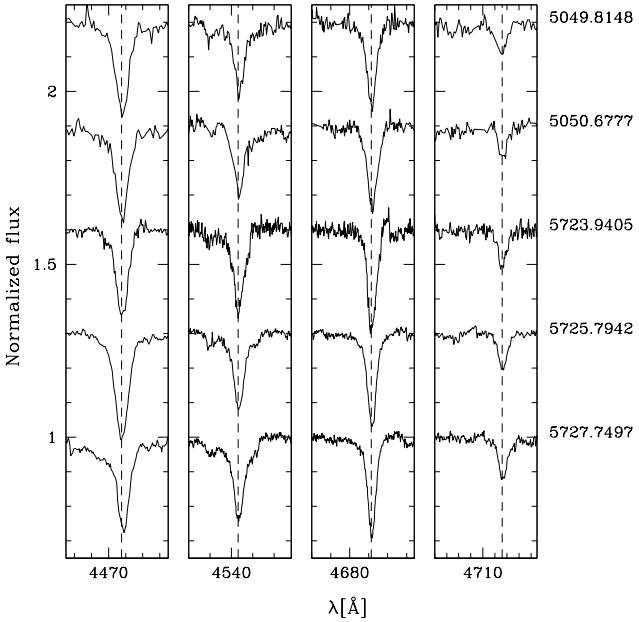

Fig. 17. The He I 4471, He II 4542, He II 4686 and He I 4713 line profiles of HD 227245.

The spectrum of HD 227245 exhibits He II slightly weaker than He I, indicating a mid O-type star. We obtain $\log W' = -0.034$ and $\log W'' = 0.218$, corresponding to a spectral type O 7III. However, the weak N III 4634–41 lines coupled with a strong He II 4686 line suggest an ((f)) suffix, indicating rather a main-sequence luminosity class. This difference could come either from the definition of the continuum level in the normalized spectra or because Conti's criterion is barely applicable to this spectral type. Therefore, we classify HD 227245 as an O 7V–III((f)) star. This spectral classification is in agreement with that given by Garmany & Vacca (1991).

4.1.4. HD 227757

HD 227757 (V = 9.25) was reported by Garmany & Stencel (1992) and Herrero et al. (1992) to be an O 9.5V star. From six spectra taken between Jun 2009 (HJD = 4988.8797) and Jun 2011 (HJD = 5728.7408), we do not observe significant variations in the RVs of HD 227757 on short nor on long timescales (see Fig. 18). Indeed, we measure $\overline{\mathrm{RVs}} = -26.8 \pm 4.6, -26.2 \pm 4.5, -28.7 \pm 2.9$ and -30.0 ± 4.3 km s^{-1} for the He I 4471, He II 4542, He II 4686 and He I 4713 lines, respectively. We thus consider the star as presumably single.

The spectrum of HD 227757 displays a stronger He I 4471 line than the He II 4542 line, indicating a spectral type (Walborn

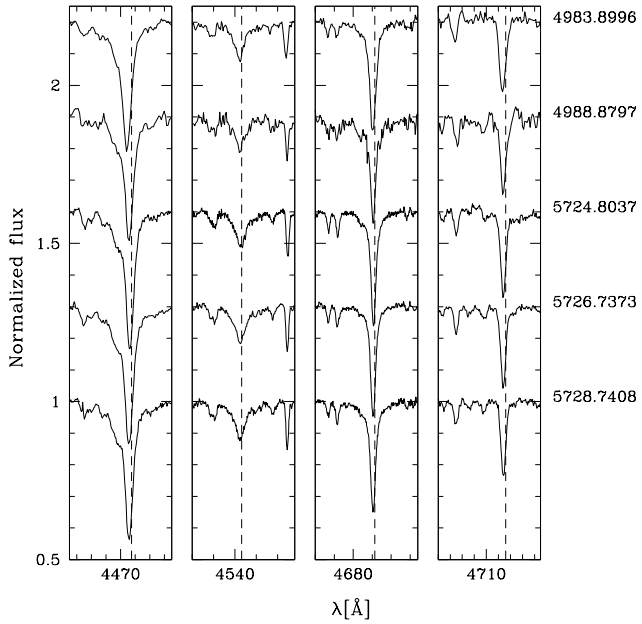

Fig. 18. The He I 4471, He II 4542, He II 4686 and He I 4713 line profiles of HD 227757.

& Fitzpatrick 1990) later than O 7. Due to the late subtype and the small $v \sin i$ of the star ($\sim$ 45 km s^{-1}), we can clearly distinguish an O II line blended with the He I 4471 line. By removing the contribution of the former line (i.e., by fitting two Gaussian profiles, one on the O II line and one on the He I line), we measure $\log W' = 0.332$, corresponding to an O 9 star. We also obtain $\log W'' = 0.081$ and $\log W''' = 5.485$ which indicate a main-sequence luminosity class (V). Therefore, we classify HD 227757 as O 9V.

5. O-type stars in the Cyg OB8 association

5.1. Presumably single stars

5.1.1. HD 191423

Better known under the name of Howarth's star, HD 191423 is the fastest rotator known to date among Galactic O stars and it was quoted as the prototype of the ONn stars (nitrogen-rich O star with broad diffuse lines, Walborn 2003). Its projected rotational velocity was estimated to be around 400 km s^{-1} (e.g., Penny & Gies 2009 computed a $v \sin i$ in the range of [336 – 436] km s^{-1}).

We obtained nine spectra of this star between Aug 2004 (HJD = 3247.3339) and Aug 2010 (HJD = 5421.5876). From the Fourier transform method of Simón-Díaz & Herrero (2007), we determine $v \sin i$ = 410 km s^{-1}, in good agreement with previous estimates. Moreover, we see in the time series of the spectra (shown in upper panels of Fig. 19) that the line widths remain constant as a function of time, thereby suggesting rather a rapid rotator than a binary system. The RVs measured by least-square fit give us average values of $\overline{\mathrm{RVs}} = -44.0 \pm 3.0, -58.8 \pm 18.4, -48.7 \pm 5.0$ and -56.5 ± 4.8 km s^{-1} for the He I 4471, He II 4542, He II 4686 and He I 4713 lines, respectively. The RV uncertainties for rapid rotators are typically larger because the centroids of the lines are not well defined. This could explain the large standard deviation observed for the weak He II 4542 line whilst the other lines are rather stable in RV, thereby indicating a pre-

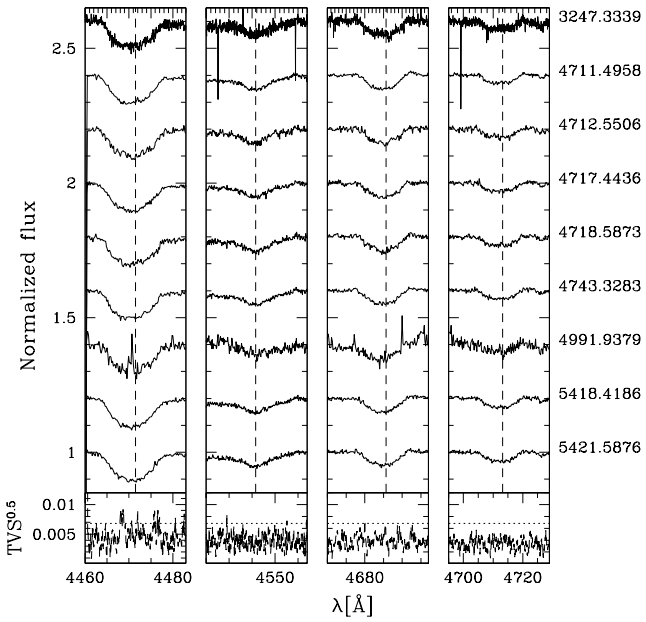

Fig. 19. Same as Fig. 8 but for HD 191423.

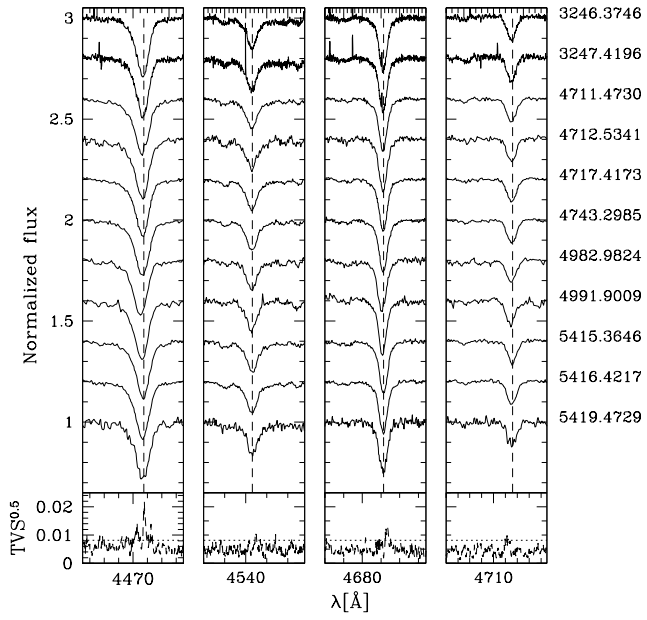

Fig. 20. Same as Fig. 8 but for HD 191978.

sumably single star. Moreover, after having computed the TVS spectra for these characteristic lines only from the Aurélie data (lower panels of Fig. 19), we detect no significant variation of line profiles, which agrees with the likely single nature of HD 191423.

Therefore, we compute $\log W' = 0.396$ and $\log W''' = 5.187$, assigning to this star an O 9III type. We are not able to estimate $\log W''$ given the blend of the Si IV 4089 line with Hδ. We also add the suffixes *n* and N, because of the broadness of the lines as well as the strong relative intensity of the nitrogen lines, thereby giving an ON 9IIIn spectral classification for HD 191423.

5.1.2. HD 191978

HD 191978 was classified as an O 8 star by Goy (1973). The investigation of its RVs by Abt & Biggs (1972) did not reveal any significant variations.

We collected eleven spectra of HD 191978 over a timescale of about 2170 days between Aug 2004 (HJD = 3247.4196) and Aug 2010 (HJD = 5419.4729). The measurements made on these data show relatively constant RVs. We can see in the upper panels of Fig. 20 that no clear Doppler shift exists relative to the rest wavelengths of four spectral lines. The mean RVs and their standard deviations are $\overline{RV} = -18.1 \pm 3.9$ km s^{-1} for the He I 4471 line, $\overline{RV} = -10.4 \pm 5.3$ km s^{-1} for the He II 4542 line, $\overline{RV} = -9.5 \pm 5.0$ km s^{-1} for the He II 4686 line, and $\overline{RV} = -11.8 \pm 6.2$ km s^{-1} for the He I 4713 line. However, the TVS spectra (lower panels of Fig. 20) indicate significant line profile variations for the He I 4471 and marginal ones for the He II 4686 line, whilst insignificant line profile variations are found for the He II 4542 and He I 4713 lines. Since these variations are not detected in all the line profiles, it is not likely that they are linked to binarity. Therefore, we consider this star as presumably single. The determinations of the EWs for the diagnostic lines yield $\log W' = 0.120$, $\log W'' = 0.227$ and $\log W''' = 5.398$, which correspond to an O 8III star.

5.1.3. HD 193117

As several O stars in our sample, HD 193117 has received little attention in the past years. We obtained eight spectra between Sep 2008 (HJD = 4711.5245) and Aug 2010 (HJD = 5420.6211). Quoted as an O 9.5II by Goy (1973), this star does not present any significant variations in its RVs. This can be seen in the upper panel of Fig. 21. We indeed measure $\overline{RVs} = -29.1 \pm 2.4$, -16.6 ± 7.1, -13.5 ± 4.8 and -26.0 ± 4.7 km s^{-1} for the He I 4471, He II 4542, He II 4686 and He I 4713 lines, respectively. In addition to these results, the TVS (lower panels of Fig. 21) shows no significant change in the line profiles of the star. Since we find no direct evidence of variations in the spectrum of HD 193117, we report this star as presumably single.

The diagnostic line ratios, He I 4471–He II 4542 and Si IV 4089–He I 4143, give $\log W' = 0.343$ and $\log W'' = 0.256$. These results correspond to an O 9III star. Furthermore, we computed $\log W''' = 5.155$ which agrees with this spectral classification.

6. O-type stars in the Cyg OB9 association

6.1. Gravitationally bound systems

6.1.1. HD 194649

Often quoted as an O 6.5 star, HD 194649 was reported by Muller (1954) to be a binary system. However, no orbital solution is found in the literature. Our dataset is composed of seventeen spectra taken between Jun 2009 (HJD = 4992.8930) and Sep 2011 (HJD = 5820.6424). These data reveal a clear SB2 signature with a secondary component moving in anti-phase relative to the primary. This motion is clearly observed over two consecutive nights, indicating a short-period binary system. By applying the Fourier method of HMM to the RVs refined by the disentangling programme, we derive an orbital period of 3.39294 ± 0.00139 days. As we did for the previous binary systems, we compute two orbital solutions: an eccentric one and a circular one. However, the best orbital solution (i.e., with the

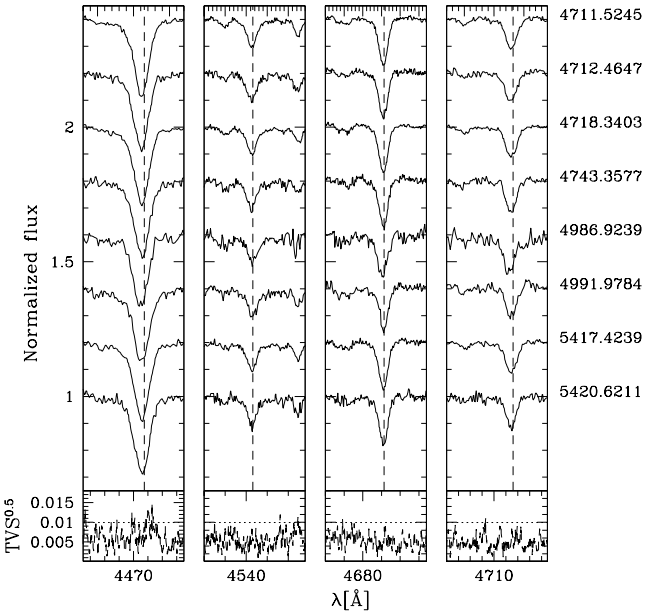

Fig. 21. Same as Fig. 8 but for HD 193117.

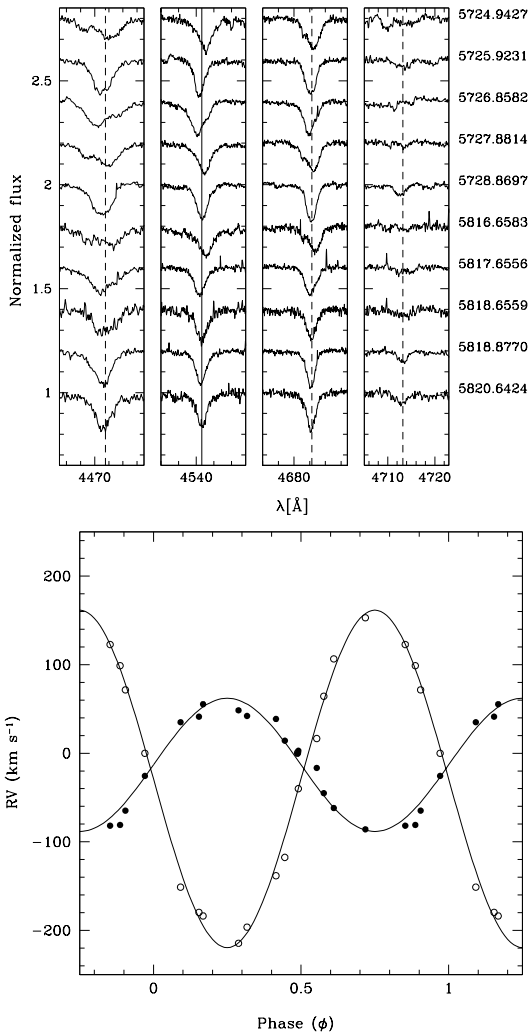

Fig. 22. *Top:* He I 4471, He II 4542, He II 4686, He I 4713 line profiles at different epochs. *Bottom:* RV curves of HD 194649 computed from $P_{\rm orb}$ = 3.39294 days. Filled circles represent the primary whilst the open circles correspond to the secondary.

smallest rms) is achieved for a circular orbit. The orbital parameters from this solution are given in Table 3 and the RV curves are shown in Fig. 22. The primary appears to be significantly more massive than the secondary. Moreover, we have a difference of about 16 km s^{-1} between the systemic velocities of both components. This discrepancy could indicate that the secondary lines are more affected by the velocity field of a strong stellar wind, although such an interpretation is at odds with the spectral types derived below which suggest an earlier and more evolved primary star.

We measure the EWs to determine the spectral classification on the disentangled and observed spectra. We find $\log W' = -0.267$ and $\log W' = 0.124$ for the primary and secondary components, respectively, corresponding to O 6 and O 8 subtypes. For the primary, it is not possible to compute $\log W''$ because the star is too early for Conti's criterion. Therefore, by focusing on the disentangled spectra (not yet corrected for the brightness ratio), the rather moderate N III 4634–41 and He II 4686 lines suggest to add an (f) tag to the primary spectral type, thus suggesting a giant luminosity class. For the secondary, we determine $\log W'' = -0.03$, corresponding to a main-sequence star (V). We thus conclude that the spectral classifications for both stars are O 6III(f) and O 8V for the primary and the secondary, respectively. On the basis of these spectral classifications, we derive a brightness ratio of about 4.7 ± 0.4, which agrees with a primary star more evolved than its companion. Finally, we use this brightness ratio to correct the individual spectra obtained by disentangling. The resulting spectra are displayed in Fig. 23.

From such spectral classifications, the tables of Martins et al. (2005) indicate radii and masses of 15 $R_\odot$ and 35 $M_\odot$ for an O 6III(f) star and of 8 $R_\odot$ and 21 $M_\odot$ for an O 8V star. From these masses and the minimum values provided in Table 3, we compute an inclination between 26° and 32° for the system. Furthermore, we determine, on the basis of Eggleton (1983), $RRL \sin i$ of 8.3 $R_\odot$ and 5.4 $R_\odot$ for the primary and the secondary, respectively, thereby giving a radius between 16 $R_\odot$ and 19 $R_\odot$ for the primary Roche lobe and between 10 $R_\odot$ and 12 $R_\odot$ for the secondary one. If the standard values are close to those of both stars, it thus appears unlikely that both components of HD 194649 fill their Roche lobe.

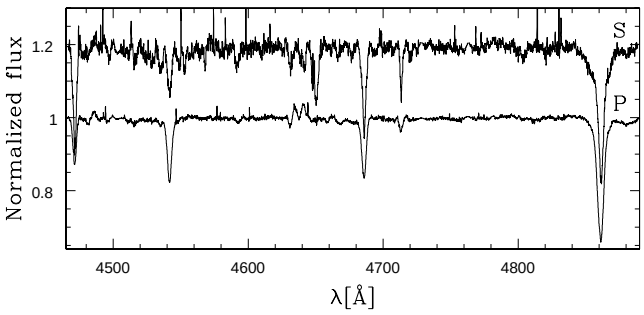

Fig. 23. Disentangled spectra of the two components of HD 194649. The spectra are normalized accounting for the brightness ratio of 4.7. The secondary spectrum is vertically shifted for clarity.

6.2. Presumably single stars

6.2.1. HD 194334

HD 194334 was classified as an O 7.5V star by Goy (1973). We collected eleven spectra between Sep 2008 (HJD = 4711.5581) and Aug 2010 (HJD = 5420.4943). We compute $\overline{RVs}$ = -15.3 ± 4.6, -3.8 ± 5.2, 23.1 ± 12.7 and -15.6 ± 5.3 km s^{-1}, for the He I 4471, He II 4542, He II 4686 and He I 4713 lines, respectively. These velocities reveal a significant variability in the He II 4686 line while the other lines are rather constant (upper panels of Fig. 24). The mean RV of the He II 4686 line is positive whilst the others are negative. This could suggest that this line is formed in the wind. Moreover, changes in certain line profiles are also detected in the TVS spectra (lower panels of Fig. 24), as notably for the He I 4471 and He II 4686 lines. However, no similar change is observed in the He II 4542 and He I 4713 lines, which strengthens the assumption that these variations are likely produced in the stellar wind. By assuming that HD 194334 is a single star, we determine $\log W' = -0.002$ and $\log W'' = 0.294$, thus giving for HD 194334 an O 7–7.5III spectral classification. The luminosity class is confirmed by Walborn's criterion. Indeed, the spectrum of HD 194334 shows moderate N III 4634–41 emissions and He II 4686 absorption lines, thereby suggesting a giant luminosity class. Therefore, HD 194334 is classified as an O 7-O 7.5III(f) star.

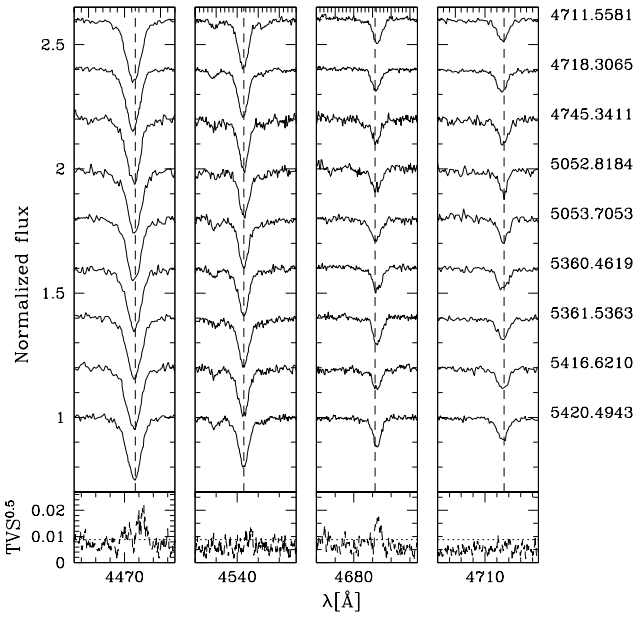

Fig. 24. Same as Fig. 8 but for HD 194334.

6.2.2. HD 195213

Reported as an O 7 star by Goy (1973), HD 195213 has been observed ten times during our campaign between Sep 2008 (HJD = 4711.5962) and Aug 2010 (HJD = 5420.5309). Our data do not reveal any significant variations of the Doppler shifts for the main lines (see upper panels of Fig. 25). We indeed compute $\overline{RVs}$ = 2.1 ± 4.5, 9.6 ± 4.6 and -2.0 ± 4.2 km s^{-1} for the He I 4471, He II 4542 and He I 4713 lines, respectively. The He II 4686 line exhibits a pattern with bf a strong emission in the line core that almost completely masks the absorption profile, thereby probably indicating that the stellar wind of the star is relatively strong. We detect, through the TVS analysis (lower panels of Fig. 25), significant variations for the He I 4471 and He II 4686 lines. Since the TVS does not indicate line profile variations in all the lines and since the RV variations are not significant, we assume that the observed variability is likely due to the stellar wind rather than to a putative companion.

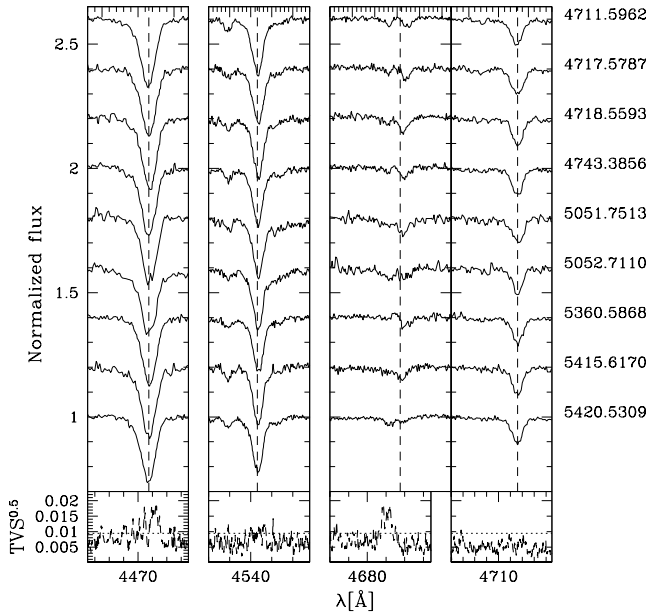

Fig. 25. Same as Fig. 8 but for HD 195213.

From the échelle spectrum, we measure $\log W' = -0.026$, corresponding to an O 7 star and $\log W'' = 0.264$, indicating a giant luminosity class (III). Moreover, we add the (f) suffix to the spectral type because the N III 4634–41 emissions are strong whilst the He II 4686 absorption is rather weak. We thus suggest an O 7III(f) spectral classification for this star.

7. Discussion

7.1. Observational biases

We performed Monte-Carlo simulations to estimate the probability to detect binary systems on the basis of our temporal sampling, for the 15 presumably single stars. For that purpose, we randomly draw the orbital parameters of 100000 binary systems. We consider that these systems are not detected if the standard deviation of the RVs is smaller than 7 – 8 km s^{-1} to be consistent with our binarity criterion. For the fast rotators, we request standard deviations of at least 15 km s^{-1}. The period distribution is chosen to be bi-uniform in log scale as in Sana et al. (2009). Under this assumption, $\log P$ is following a bi-uniform distribution between 0.3 and 1.0 for 60% of the systems and between 1.0 and 3.5 for the remaining 40%. The eccentricities are selected uniformly between 0.0 and 0.9. As Rauw et al. (2011) already did, we assume that, for orbital periods shorter than 4 days, the systems have circular orbits. Indeed, with such periods, the circularization of systems composed of O-type stars is generally already done or almost achieved. The mass ratio (M_P/M_S) is uniformly distributed between 1.0 and 10.0 and the mass of the pri-

Table 3. Orbital solutions for the four newly-detected binary systems

Parameters	HD 193443		HD 228989		HD 229234	HD194649	
	Primary	Secondary	Primary	Secondary	Primary	Primary	Secondary
P [d]	7.467 ± 0.003		1.77352 ± 0.00041		3.51059 ± 0.00175	3.39294 ± 0.00139	
e	0.315 ± 0.024		0.0		0.0	0.0	
ω [°]	289.7 ± 5.8						
T_0 (HJD)	3246.120 ± 0.106		5047.771 ± 0.003		4714.326 ± 0.011	4991.082 ± 0.009	
γ [km s^{-1}]	-10.0 ± 1.2	-16.6 ± 2.0	−3.7 ± 1.8	−7.8 ± 1.9	-16.3 ± 0.8	-13.8 ± 2.1	-29.5 ± 3.1
K [km s^{-1}]	38.8 ± 1.5	91.3 ± 3.4	194.3 ± 2.5	220.3 ± 2.9	48.5 ± 1.1	76.3 ± 2.5	192.1 ± 6.2
$a \sin i$ [$R_\odot$]	5.4 ± 0.2	12.8 ± 0.5	6.8 ± 0.1	7.7 ± 0.1	3.4 ± 0.1	5.1 ± 0.2	12.9 ± 0.4
$M \sin^3 i$ [$M_\odot$]	1.0 ± 0.1	0.4 ± 0.1	7.0 ± 0.2	6.1 ± 0.2		4.9 ± 0.4	1.9 ± 0.1
q (M_P/M_S)	2.35 ± 0.11		1.13 ± 0.02			2.52 ± 0.13	
f_{mass} [$M_\odot$]					0.042 ± 0.003		
rms [km s^{-1}]	5.08		8.37		3.04	11.13	

Notes. The 1-σ error-bars on the parameters are provided by LOSP, except for the orbital period whose uncertainty is determined on the basis of the natural width of the peaks in the Fourier power spectrum. The orbital solution of HD 193443 was computed assuming that the uncertainties on the secondary RVs are three times as large as for the primary.

mary is obtained from tables of Martins et al. (2005) according to the spectral classification of the star. The longitudes of periastron are uniformly drawn between 0 and 2π, and the orbital inclinations are randomly drawn according to $\cos i \in [-1; 1]$ from a uniform distribution.

Table 4. Binary detection probability (%) for the time sampling associated to the different presumably single stars in our sample and for various period ranges (expressed in days).

Stars	Short	Intermed.	Long	All
	[2 − 10]	[10 − 365]	[365 − 3165]	[2 − 3165]
HD 193514	99.8	96.0	84.1	94.1
HD 193595	99.7	86.6	64.5	86.6
HD 193682	99.8	92.4	73.6	90.2
HD 194094	99.2	87.0	68.8	87.8
HD 194280	99.9	96.0	85.1	94.5
HD 228841	99.0	81.4	44.3	78.8
HD 190864	99.9	94.5	76.0	91.2
HD 227018	99.8	82.9	57.1	84.0
HD 227245	99.5	68.3	59.5	83.9
HD 227757	99.5	82.4	63.3	86.0
HD 191423	98.8	72.3	36.5	75.6
HD 191978	99.8	94.1	79.5	92.4
HD 193117	99.8	91.0	72.1	89.5
HD 194334	99.7	91.3	63.3	86.4
HD 195213	99.7	89.2	67.9	88.0

The results of these simulations are listed in Table 4. This table gives the percentage of systems that would be detected with the same temporal sampling as our survey if their orbital period was short, intermediate, long or covering a timescale going from 2 to more than 3000 days, respectively. This reveals that at least 72% of the systems with periods smaller than one year should have been detected. However, between 11 and 64% of the systems with an orbital period larger than one year could have been missed. These results show that the detection efficiency of our survey is rather good, especially for systems with periods shorter than one year, but that we may also have missed some of the long-period binary systems. These results thus emphasize that the short-period systems are easier to detect than the long-period systems with this strategy of observation.

7.2. Binary fraction in Cygnus OB associations

The spectroscopic analysis made on the Cygnus region includes O-type stars coming from different environments. Therefore, considering them altogether boils down to study a random sample of O-stars. It is also possible to focus on each association or even on young open clusters belonging to these associations. However, in the latter case, we would deal with small number statistics. The binary fraction will thus be discussed both over the entire region and for each OB association.

We observed nineteen stars or multiple systems containing at least one O-type object. Among this sample, one star, HD 229234, was classified as SB1 and three were reported as SB2 systems, HD 193443, HD 194649 and HD 228989. Therefore, no doubt remains on the binary status of these objects. As a first step, we focus on each individual OB association by first including only our sample stars. In Cyg OB1, the minimal binary fraction is of 33% (3 stars out of 9). In Cyg OB3, we find no star in a binary system out of 4, i.e., 0% whilst in Cyg OB8 and Cyg OB9, we obtain 0% (0 out of 3) and 33% (1 out of 3), respectively. By putting together these numbers to achieve a more global view of our sample, we find a minimum binary fraction of about 21% among the nineteen sample stars (4 out of 19). However, if we take into account all the O stars mentioned by Humphreys (1978), the minimum O-type star binary fractions become equal to 33% (4 out of 12, BD +36 4063 also detected as binary with P_{orb} = 4.8 days, Williams et al. 2009), 33% (3 out of 9, HD 191201, Burkholder et al. 1997, HD 190918, Hill & Underhill 1995, and HD 226868, Gies & Bolton 1982, were detected as binaries with orbital periods of 8.3, 112.4, 5.6 days, respectively), 0% (0 out of 4) and 14% (1 out of 7) for the Cyg OB1, Cyg OB3, Cyg OB8 and Cyg OB9 associations, respectively. Overall, we thus obtain a minimal binary fraction of 25% (8 stars out of 32). Of course, this value was determined by focusing only on the Cyg OB1, Cyg OB3, Cyg OB8 and Cyg OB9 associations and is therefore not representative of the entire Cygnus region. Therefore, we include in this discussion the results of the large spectroscopic/photometric survey of Kiminki & Kobulnicky (2012, and the subsequent papers). These authors have indeed analysed 114 stars belonging to the Cyg OB2 association. This sample takes into account massive objects for which the primary stars are classified between B 3 and O 5. They found a hard minimum binary fraction of 21% (24 out of 114). Although our sample is clearly smaller, the min-

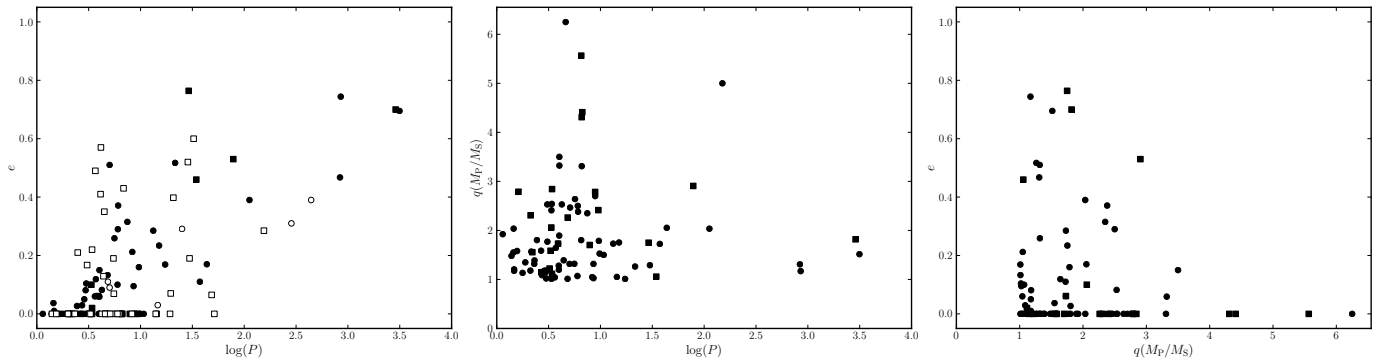

Fig. 26. Distributions of orbital parameters (period, eccentricity, mass ratio) of binary systems located in young open clusters or OB associations.

imum binary fraction appears to be similar in most of the OB associations in the Cygnus complex. Finally, putting all these results together, we reach a general minimum binary fraction of 22% (32 out of 146) in the Cygnus region.

7.3. Massive binaries in a wider context

To bring additional constraints to this work in a larger frame, we have selected the SB1 and SB2 systems (including at least one O star) detected in various spectroscopic multiplicity studies (Sana et al. 2008, 2009, 2011; Rauw & De Becker 2004; De Becker et al. 2006; Hillwig et al. 2006; Rauw et al. 2009; Mahy et al. 2009) as well as in numerous papers (see, e.g., "spectroscopic" references in Mason et al. 1998) including studies devoted to the Cyg OB2 association (Rauw et al. 1999; De Becker et al. 2004; Nazé et al. 2008; Kiminki et al. 2012, and the subsequent papers). Finally, we complete this dataset by adding the orbital information concerning the O-type stars provided by the 9th spectroscopic binary catalogue (Pourbaix et al. 2004). Orbital solutions are then known for more than 140 systems (SB1[2] and SB2) which are mainly located in young open clusters or OB associations. We present, in Fig. 26, the corresponding P vs. e, P vs. q (= M_P/M_S) and q vs. e diagrams. In this figure, the filled symbols represent the SB2s, the open ones the SB1 systems, and the squares give the parameters quoted in the 9th spectroscopic binary catalogue. In order not to affect the readibility of these diagrams and because some are missing, we do not include the error-bars on these measurements.

From the period-eccentricity diagram (left panel of Fig. 26), we see that shorter period systems are dominantly characterized by lower eccentricities, suggesting a lack of highly eccentric short period systems as well as almost circular long period systems. The majority of the datapoints seems to show a trend between the period and the eccentricity. However, the question of the completeness of the data has to be asked. Indeed, Sana & Evans (2011) mentioned that at least half the known and suspected spectroscopic binaries lack a reliable orbital solution. Among the systems that lack a reliable solution, the majority has long orbital periods. The apparent linear trend between eccentricity and orbital period could be affected by two competing observational biases. Indeed, highly eccentric SB2 systems display large RV separations at periastron which are easier seen than the lower RV excursions of circular systems. However the duration over which these large separations are observed is rather short and could easily be missed.

[2] SB1 systems have not been included in the P vs. q and q vs. e plots because of the difficulty to infer reliable mass ratios in such systems.

We see from the P vs. q plot (middle panel of Fig. 26) that the majority of detected systems are those with a period smaller than 30 days and with a mass ratio between 1 and 3. This plot does not agree with a uniform distribution of the mass ratios in the range $1 < q < 5$ as Sana & Evans (2011) suggested it. However, these authors also reported a decrease of the number of systems with $q > 1.7$ as it can be see in Fig. 26. These results clearly show the limitations of spectroscopy. Indeed, it is hardly possible to detect a secondary signature for systems with large mass differences without having high-quality high signal-to-noise data.

Finally, the q vs. e plot (right panel of Fig. 26) shows that a larger amount of systems with small eccentricities have mass ratios between 1 and 3 or said differently that only systems with almost similar components display a small eccentricity. However, the detectability of systems with a high mass ratio or a high eccentricity is difficult. Our sample could thus be biased. The decreasing range of high eccentricities for higher mass ratios, observed in the right panel of Fig. 26 could thus likely be stemmed from decreasing completeness, making this conclusion less reliable. Indeed, the time required for the circularization, given by Hurley et al. (2002), is dependent on the mass ratio ($q = (M_P/M_S)$) squared. Therefore, when q is very high, the theory predicts that the time to circularize the system will be larger, which is not the case here.

Although this sample remains small in comparison to the overall population of binaries among the O-type stars, these three diagrams provide a first approximation of the general distribution of orbital parameters. It would be interesting however to include in these diagrams binaries which would be detected by adaptive optics, speckle interferometry or interferometry to cover larger orbital parameter distributions.

8. Conclusion

We revisited the binary status of nineteen O-type stars located in different OB associations of the Cygnus region. We confirm the binarity of four objects, three SB2s: HD 193443, HD 194649, HD 228989 and one SB1: HD 229234. All these systems have short-term orbital periods, less than 10 days. We also derived for the first time the orbital parameters for the three SB2 systems. The apparent lack of intermediate and long period systems in these OB associations contrasts with the case of the NGC 2244 young open cluster where only one longer period system HD 46149 has been identified (HD 46573 being located in Mon OB2 association and not in NGC 2244, Mahy et al. 2009). However, this difference seems linked to the sample. Indeed, among the four stars belonging to Cygnus OB associations which were already known as binaries and thus not in-

cluded in our sample, HD 190918 is also a long period binary ($P_{\rm orb}$ = 112.4 days, Hill & Underhill 1995). This result therefore does not allow us to point to different conditions for massive star formation.

The stars contained in our sample were chosen because of their brightness and because, for most of them, their binary status has not yet been established. These nineteen stars thus constitute a random sample of O-type stars. Our strategy of observations allowed us to reach a binary detection rate close to 90% for periods up to 3165 days and to determine a minimum spectroscopic binary fraction in this sample of 21%. By including the stars of Humphreys' catalogue (1978) which belong to the OB associations studied in the present paper but which were not analysed because their binarity was already known, we reach a minimum spectroscopic binary fraction of 25%. When we consider all these associations separately, we obtain 33% of O-type stars in binary systems in Cyg OB1, 33% in Cyg OB3, 0% in Cyg OB8 and 14% in Cyg OB9. All these values can be completed by the minimum binary fraction of 21% quoted by Kiminki & Kobulnicky (2012) in Cyg OB2. Finally, when we take all these binary fractions together, we reach a binary fraction for the Cygnus region of about 22% (32 stars out of 146).

In addition to the analysis of the RV variations, several objects show significant variations of their line profiles. These variations are mainly observed for the He I 4471 and He II 4686 lines. Since not all the lines are affected, this implies that these variations are probably not due to binarity but rather result from phenomena intrinsic to stellar winds or perhaps even from non-radial pulsations. The spectral classifications of the stars derived in the present paper and the results of the TVS analysis are summarized in Table 5.

The results presented here only focus on a small sample of O-type stars in the Cygnus complex. This region represents a large panel of O-type stars which can provide numerous clues on the formation scenarios of these objects. In paper II, we will continue the analysis of these stars by determining with a model atmosphere code their individual parameters, their age, and their chemical enrichment to better constrain the properties of these objects.

Acknowledgements. We thank the anonymous referee for useful remarks and comments. This research was supported by the PRODEX XMM/Integral contract (Belspo), the Fonds National de la Recherche Scientifique (F.N.R.S.) and the Communauté française de Belgique – Action de recherche concertée – A.R.C. – Académie Wallonie-Europe. We also thank the staff of San Pedro Màrtir Observatory (Mexico) and of Observatoire de Haute-Provence (France) for their technical support. The SIMBAD database has been consulted for the bibliography.

References

Abt, H. A. & Biggs, E. S. 1972, Bibliography of stellar radial velocities (Kitt Peak National Observatory, Tucson)
Boeche, C., Munari, U., Tomasella, L., & Barbon, R. 2004, A&A, 415, 145
Burkholder, V., Massey, P., & Morrell, N. 1997, ApJ, 490, 328
Comerón, F., Pasquali, A., Rodighiero, G., et al. 2002, A&A, 389, 874
Conti, P. S. 1973, ApJ, 179, 161
Conti, P. S. & Alschuler, W. R. 1971, ApJ, 170, 325
Conti, P. S. & Ebbets, D. 1977, ApJ, 213, 438
Conti, P. S. & Leep, E. M. 1974, ApJ, 193, 113
Conti, P. S., Leep, E. M., & Lorre, J. J. 1977, ApJ, 214, 759
De Becker, M., Rauw, G., & Manfroid, J. 2004, A&A, 424, L39
De Becker, M., Rauw, G., Manfroid, J., & Eenens, P. 2006, A&A, 456, 1121
Eggleton, P. P. 1983, ApJ, 268, 368
Forbes, D. 1981, PASP, 93, 441
Fullerton, A. W., Gies, D. R., & Bolton, C. T. 1996, ApJS, 103, 475
García, B. & Mermilliod, J. C. 2001, A&A, 368, 122
Garmany, C. D. & Stencel, R. E. 1992, A&AS, 94, 211
Garmany, C. D. & Vacca, W. D. 1991, PASP, 103, 347
Gies, D. R. & Bolton, C. T. 1982, ApJ, 260, 240
González, J. F. & Levato, H. 2006, A&A, 448, 283
Gosset, E., Royer, P., Rauw, G., Manfroid, J., & Vreux, J.-M. 2001, MNRAS, 327, 435
Goy, G. 1973, A&AS, 12, 277
Hanson, M. M. 2003, ApJ, 597, 957
Heck, A., Manfroid, J., & Mersch, G. 1985, A&AS, 59, 63
Herrero, A., Kudritzki, R. P., Vilchez, J. M., et al. 1992, A&A, 261, 209
Hill, G. M. & Underhill, A. B. 1995, in IAU Symposium, Vol. 163, Wolf-Rayet Stars: Binaries; Colliding Winds; Evolution, ed. K. A. van der Hucht & P. M. Williams, 235
Hillwig, T. C., Gies, D. R., Bagnuolo, Jr., W. G., et al. 2006, ApJ, 639, 1069
Hiltner, W. A. 1956, ApJS, 2, 389
Humphreys, R. M. 1978, ApJS, 38, 309
Hurley, J. R., Tout, C. A., & Pols, O. R. 2002, MNRAS, 329, 897
Kiminki, D. C. & Kobulnicky, H. A. 2012, ApJ, 751, 4
Kiminki, D. C., Kobulnicky, H. A., Ewing, I., et al. 2012, ApJ, 747, 41
Knödlseder, J., Cerviño, M., Le Duigou, J.-M., et al. 2002, A&A, 390, 945
Liu, T., Janes, K. A., & Bania, T. M. 1989, AJ, 98, 626
Mahy, L., Nazé, Y., Rauw, G., et al. 2009, A&A, 502, 937
Maíz-Apellániz, J., Walborn, N. R., Galué, H. Á., & Wei, L. H. 2004, ApJS, 151, 103
Malchenko, S. L. & Tarasov, A. E. 2009, Astrophysics, 52, 235
Martins, F., Schaerer, D., & Hillier, D. J. 2005, A&A, 436, 1049
Mason, B. D., Gies, D. R., Hartkopf, W. I., et al. 1998, AJ, 115, 821
Mason, B. D., Hartkopf, W. I., Gies, D. R., Henry, T. J., & Helsel, J. W. 2009, AJ, 137, 3358
Massey, P., Johnson, K. E., & Degioia-Eastwood, K. 1995, ApJ, 454, 151
Mathys, G. 1988, A&AS, 76, 427
Mathys, G. 1989, A&AS, 81, 237
Meisel, D. D. 1968, AJ, 73, 350
Mel'Nik, A. M. & Efremov, Y. N. 1995, Astronomy Letters, 21, 10
Morgan, W. W., Code, A. D., & Whitford, A. E. 1955, ApJS, 2, 41
Muller, P. 1954, AJ, 59, 388
Nazé, Y., De Becker, M., Rauw, G., & Barbieri, C. 2008, A&A, 483, 543
Negueruela, I. 2004, Astronomische Nachrichten, 325, 380
Nelan, E. P., Walborn, N. R., Wallace, D. J., et al. 2004, AJ, 128, 323
Penny, L. R. & Gies, D. R. 2009, ApJ, 700, 844
Penny, L. R., Gies, D. R., Hartkopf, W. I., Mason, B. D., & Turner, N. H. 1993, PASP, 105, 588
Plaskett, J. 1924, Publications of the Dominion Astrophysical Observatory Victoria, 2, 286
Pourbaix, D., Tokovinin, A. A., Batten, A. H., et al. 2004, A&A, 424, 727
Rauw, G. & De Becker, M. 2004, A&A, 421, 693
Rauw, G., Nazé, Y., Fernández Lajús, E., et al. 2009, MNRAS, 398, 1582
Rauw, G., Sana, H., Gosset, E., et al. 2000, A&A, 360, 1003
Rauw, G., Sana, H., & Nazé, Y. 2011, A&A, 535, A40
Rauw, G., Vreux, J.-M., & Bohannan, B. 1999, ApJ, 517, 416
Reipurth, B. & Schneider, N. 2008, in ASP Monograph Publications, Vol. 4,Handbook of Star Forming Regions, Vol. I: The Northern Sky, ed. B. Reipurth (San Francisco: ASP), 36
Repolust, T., Puls, J., & Herrero, A. 2004, A&A, 415, 349
Sana, H. & Evans, C. J. 2011, in IAU Symposium, Vol. 272, IAU Symposium, ed. C. Neiner, G. Wade, G. Meynet, & G. Peters, 474
Sana, H., Gosset, E., & Evans, C. J. 2009, MNRAS, 400, 1479
Sana, H., Gosset, E., Nazé, Y., Rauw, G., & Linder, N. 2008, MNRAS, 386, 447
Sana, H., Gosset, E., & Rauw, G. 2006, MNRAS, 371, 67
Sana, H., James, G., & Gosset, E. 2011, MNRAS, 416, 817
Schmidt-Kaler. 1982, in Landolt-Börnstein new series VI, ed. K. Schaifers & H. M. Voight, Vol. 2b, (New York: Springer-Verlag), 15
Simón-Díaz, S. & Herrero, A. 2007, A&A, 468, 1063
Sota, A., Maíz Apellániz, J., Barbá, R. H., et al. 2011, Bulletin de la Société Royale des Sciences de Liège, 80, 519
Turner, N. H., ten Brummelaar, T. A., Roberts, L. C., et al. 2008, AJ, 136, 554
Underhill, A. B. 1994, ApJ, 420, 869
Underhill, A. B. 1995, ApJS, 100, 433
Uyanıker, B., Fürst, E., Reich, W., Aschenbach, B., & Wielebinski, R. 2001, A&A, 371, 675
Walborn, N. R. 1971, ApJS, 23, 257
Walborn, N. R. 2003, in Astronomical Society of the Pacific Conference Series, Vol. 304, Astronomical Society of the Pacific Conference Series, ed. C. Charbonnel, D. Schaerer, & G. Meynet, 29–+
Walborn, N. R. & Fitzpatrick, E. L. 1990, PASP, 102, 379, erratum: 102, 1094
Walborn, N. R. & Howarth, I. D. 2000, PASP, 112, 1446
Williams, S. J., Gies, D. R., Matson, R. A., & Huang, W. 2009, ApJ, 696, L137
Wolfe, Jr., R. H., Horak, H. G., & Storer, N. W. 1967, The machine computation of spectroscopic binary elements, in Modern Astrophysics. A memorial to Otto Struve, ed. M. Hack (New York: Gordon & Breach), 251

Table 5. Summary of the multiplicity of stars and of their line profile variations

Stars	Sp. type	TVS variations			
		He I 4471	He II 4542	He II 4686	He I 4713
HD 193443	O 9 + O 9.5	Y	Y	Y	Y
HD 193514	O 7–O 7.5 III(f)	Y	Y	Y	N
HD 193595	O 7V	Y	N	N	N
HD 193682	O 5III(f)	N	N	Y	N
HD 194094	O 8III	–	–	–	–
HD 194280	O 9.7	Y	N	N	N
HD 228841	O 7n	N	N	N	N
HD 228989	O 8.5V + O 9.7V	Y	Y	Y	Y
HD 229234	O 9III + ...	Y	Y	Y	Y
HD 190864	O 6.5III(f)	Y	N	Y	N
HD 227018	O 6.5V((f))	Y	N	N	N
HD 227245	O 7V–III((f))	–	–	–	–
HD 227757	O 9V	–	–	–	–
HD 191423	ON 9IIIn	N	N	N	N
HD 191978	O 8III	Y	N	Y	N
HD 193117	O 9III	Y	N	N	N
HD 194334	O 7–O 7.5 III(f)	Y	N	Y	N
HD 194649	O 6III(f) + O8V	Y	Y	Y	Y
HD 195213	O 7III(f)	Y	N	Y	N

Notes. Notes: “Y” means that significant TVS variations in the spectral lines are observed whilst “N” reports the absence of variations.

Wright, N. J., Drake, J. J., Drew, J. E., & Vink, J. S. 2010, ApJ, 713, 871
Zinnecker, H. & Yorke, H. W. 2007, ARA&A, 45, 481